ULTRASTRUCTURAL CHARACTERIZATION OF ULTRAVIOLET INDUCED CORNEAL DISEASE - AN ANIMAL MODEL

UNIVERSITY OF CAPE TOWN

DEPARTMENT OF ANATOMY AND CELL BIOLOGY

FACULTY OF MEDICINE

KLAUS SCHULTES

Thesis submitted towards the degree of

Master of Science

in

Medical Sciences (Cell Biology)

Supervisor: Professor W J Els

Assistant Supervisor: Dr J C Hill

Date: 1994

B. Declaration

I, Klaus Schultes hereby declare that the work on which this thesis is based is original and that neither the whole work nor any part of it has been, is being, or is to be submitted for another degree in this or any other University.

I empower the university to reproduce for the purpose of research either the whole or any portion of the contents in any manner whatsoever.

.....

Klaus Schultes
.....

C. Acknowledgements

The work for this degree was done in part at the Electron Microscopy Unit of The University of Cape Town, the Department of Medicine of the University of Cape Town and the Life Sciences Electron Microscopy Unit of McMaster University in Ontario Canada. I would like to express my gratitude to Dr Dave Crawford for giving me the opportunity to undertake this project in conjunction with my regular full time position at the Electron Microscopy Unit. In addition I would like to thank Dr Jack Hill and Dr Richard Maske for introducing me to the study of corneal diseases and for their assistance and guidance through out the experimental part of the project. A very special thanks and gratitude to my supervisor, Prof W J Els for his consistent support and patience over these past several years. Clearly, without his help and support I would no doubt have abandoned this project after leaving Cape Town.

Thank you again.

I also wish to thank the Department of Anatomy and Cell Biology, the University of Cape Town and McMaster University for financial assistance and for the use of their equipment.

TABLE OF CONTENTS

INTRODUCTION

1.1. The properties of light

In the last three hundred years the very nature of light has been at the centre of controversy as two rival theories tried to explain light's properties. Initially Isaac Newton treated light as a train of particles and put forward his corpuscular theory that for the next hundred years was widely accepted. Many observations describing the reflection and refraction of light could be explained by a model that treated light as a stream of particles. On the other side, Christopher Huygens, a Dutchman visualized light as a wavelike phenomenon. Since waves bend around obstacles and we cannot see around obstacles, it was taken as evidence against the wave theory. However, experiments in the nineteenth century demonstrated that the bending of light around objects is difficult to observe because of the short wavelength of visible light. In addition, further support for the wave theory came from the French physicist Foucault who showed by direct measurement that light does travel more slowly in a denser medium. Maxwell's work on electromagnetic radiation provided the theoretical foundation for the wave model of light. Thus, early in the 20th century it seemed that the wave theory could adequately explain most observations regarding the properties of light, except that it could not correctly describe some processes in which light is absorbed or emitted from matter.

In 1905 Albert Einstein, applying Max Planck's quantum theory showed that light not only behaved like waves, but it can also act like a stream of tiny particles when it collides with solid objects such as atoms. He worked out a mathematical picture of how an electron in metal could absorb one bit of light energy, which at that time he called a light quantum - later called a photon - and thus have the energy to escape. Then in 1923, the American physicist Arthur H. Compton demonstrated that photons have momentum, and consequently mass - strong support for Einstein's theory. Other experiments followed, showing that when light interacts with matter, events that take place can be understood only by considering light as separately packaged bits of energy. These developments were upsetting theoretical physics, though they provided the impetus that led to the development of the modern **Quantum** theory, developed by the joint efforts of the great men of modern physics.

The quantum theory states that light is composed of quanta or photons having both wavelike and particlelike traits. At times, one property predominates: at times the other predominates.

In 1801 Johann Ritter discovered the ultraviolet region of the electromagnetic spectrum. He could show that chemical action was caused by some form of energy in the dark portion beyond the violet range. Today we know that ultraviolet radiation is but a small part of the electromagnetic spectrum and lies between the visible and the X-ray regions.

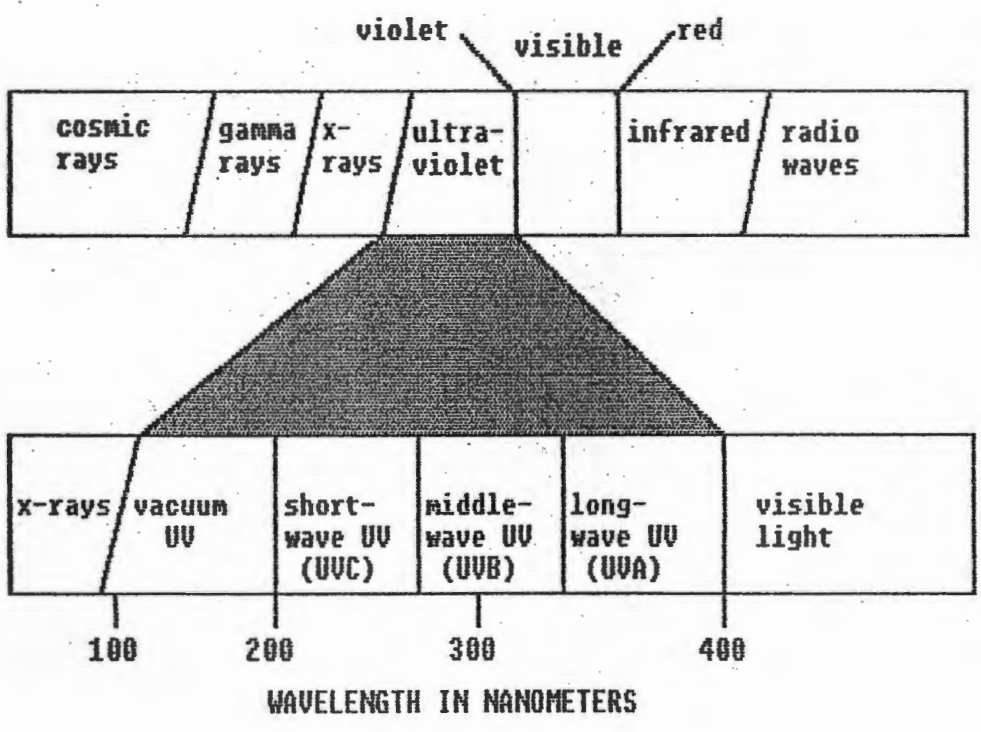

Figure 1. The electromagnetic spectrum according to Morrison (1984).

1.2. Sunlight and the electromagnetic spectrum

The sun's radiant energy has been a significant factor in the development and existence of life on earth. The spectral distribution and the total amount of radiant energy reaching the earth's surface are both important factors in our environment. At the earth's surface this spectral distribution varies considerably with the time of day and season of the year. Only about two-thirds of the radiant energy arriving at the upper atmosphere actually reaches the earth's surface, the remainder is reflected, scattered or absorbed in the atmosphere. Of this

energy 50% lies in the visible spectrum and roughly 5% in the ultraviolet region, the other 45% is made up of all the other forms of electromagnetic radiation. The solar radiation we experience is made up of a direct component (sunlight) and a diffuse or scattered component known as (skylight). Total radiation is sunlight plus skylight.

Ultraviolet radiation is but a small part of the electromagnetic spectrum, a collective term encompassing all forms of electromagnetic radiation. The physical difference between radio waves, infra red, ultraviolet and X-rays is purely the wavelength of the radiation. The relationship between energy (E) and wavelength (λ) attributes photons with energy, $E=hv$ and momentum $p=h/\lambda$ (where h is Planck's constant).

1.3. The ultraviolet spectrum

Ultraviolet radiation forms that part of the electromagnetic spectrum we know as "nonionizing radiation," an arbitrary region of wavelengths longer than 100 nm. In nonionizing radiation, the photons have insufficient energy to cause ionization of atoms in solution. Although ultraviolet radiation only occupies a small slice of the electromagnetic spectrum, it has important biological significance. The ultraviolet spectrum is also divided into three spectral regions on the basis of causing biological damage; namely **UV-A, UV-B and UV-C**. The notion was first put forward at the Copenhagen meeting of the Second International Congress on light held during August 1932. At that time the three spectral regions were defined as follows:

Spectral Region	Also known as	Range of Wavelengths
UV-A	longwave or blacklight	400 - 315 nm
UV-B	middlewave or erythemal	315 - 280 nm
UV-C	shortwave or germicidal	< 280 nm

Figure 2. Ultraviolet spectral division as defined by the Second International Congress on Light.

Internationally these recommendations have been endorsed by the International Commission on Illumination (ice), the National Institute for Occupational Safety and Health (nosh) in the United States, and the Health and Safety Executive (she) and the National Radiological Protection Board (NRPB) in the United Kingdom, with the slight modification that the lower limit of the UV-C region is taken to be 100 nm by the CIE, HSE and NRPB, and 200 nm by the NIOSH. It was the development of environmental photobiology that prompted some workers, Parrish et al. (1978) to redefine the boundaries of the three spectral regions as follows:

UV-A 400 - 320 nm
UV-B 320 - 290 nm
UV-C 290 - 200 nm

The divisions into distinct spectral regions are not necessarily rigid, though it seems sensible to follow

international recommendations. Therefore, the convention used in this thesis is that detailed in Fig. 2.

The global ultraviolet radiation we are subject to is attenuated somewhat by the following effects:

a) absorption by atmospheric ozone.

b) Rayleigh scattering due to oxygen, nitrogen and other molecular components of the atmosphere.

c) Mie scattering caused by dust, aerosols, water droplets and other particles of diameter comparable to the wavelength of radiation.

Other factors such as the degree of cloud cover and ground reflection also effect the global ultraviolet environment and ultimately the amount of ultraviolet radiation we are exposed to on a day to day basis.

1.3.1. Ultraviolet A radiation

Also known as blacklight, longwave or near UV radiation, UV-A at 400 - 315 nm is the least biologically active of the three UV spectra. When one considers biological damage as related to UV radiation, photon energy and the amount of radiation present are both important factors. We know that the energy of photons is inversely proportional to their wavelength, therefore, a UV-A photon at 390 nm has much less energy than a UV-B photon at 300 nm and consequently, it is less damaging biologically. On the other hand sunlight contains much more UV-A than UV-B, an important factor when discussing biological effects. UV-A is thought to be partially responsible for a sun induced erythema

and more directly in the formation of cataracts. Bachem (1956) concluded that solar ultraviolet (290 - 400 nm) can cause sunlight induced cataracts.

1.3.2 Ultraviolet B radiation

The most biologically active UV radiation in sunlight, UV-B at 280 - 315 nm is also known as "middlewave" or "sunburn radiation". UV-B radiation affects us significantly, firstly as a major contributor to sunburn, and secondly as the culprit in numerous corneal diseases (see section on Corneal diseases).

The intensity of the UV-B waveband is more strongly dependent on the height of the sun in the sky than the wavebands in the other two ultraviolet regions. This is due to the fact that shorter wavelengths are more prone to scattering than are longer wavelengths, consequently the greater the thickness of atmospheric molecules to be traversed, the greater the chance for wavelengths to be scattered. For this reason the sunburning effectiveness of sunlight is about 100 times more intense in the summer when the sun is higher in the sky. UV-B radiation forms a significant part of the scattered or skylight portion of the total solar radiation. In early morning and late afternoon the scattered component is significantly larger than the direct component. The importance of this scattered UV-B radiation is evident when one gets sunburnt while sitting in the shade. Equally important is surface reflection. For example, fresh snow on the ground may scatter in excess of 80% of the incident UV-B

radiation upwards. This can lead to severe burning or even snow blindness.

1.3.3 Ultraviolet C radiation

Other terms for this 200 to 240 nm waveband are "germicidal" and "shortwave" radiation. It is generally not found in sunlight at the earth's surface since UV-C radiation is mainly filtered out by the ozone layer and by water vapour in the atmosphere. Although not found at the earth's surface it is still considered biologically significant . Various artificial generators such as: high pressure mercury lamps, welding torches and certain types of fluorescent tubes emit abundant quantities of UV-C radiation. UV-C radiation has a very powerful germicidal action and is used commercially to kill microorganisms.

1.4. The ozone layer and its effect on ultraviolet radiation

The entire absence of radiation wavelengths shorter than 280 nm striking the earth's surface can be attributed to a very thin blanket of ozone in the upper atmosphere. It is concentrated well above the earth's surface between 10 to 50 kilometres with a peak at 25 kilometres. There is very little of this gas in the atmosphere and under normal conditions the ozone layer varies between a thickness of only 2.4 mm to 4.6 mm nevertheless its effects are very pronounced. The presence of the ozone layer is of vital importance to life on earth. Foremost is the capability

of ozone to absorb damaging ultraviolet radiation from the sun. The absorption of ultraviolet radiation by ozone is important for wavelengths less than 330 nm, where the values of the ozone coefficient increase rapidly with decreasing wavelength. Accordingly there is practically no radiation with wavelengths less than 295 nm which reaches the Earth's surface (most of UV-B and almost all of UV-C).

Ozone is probably concentrated where it is because of a balance between two factors: (1) the availability of shortwave ultraviolet radiation from the sun which is necessary to produce atomic oxygen and (2) an atmosphere dense enough to bring about the necessary collisions between molecular oxygen and atomic oxygen. Ozone is the triatomic form of oxygen **(O_3)** and is the marriage of an oxygen atom **(O)** with an oxygen molecule **(O_2)**. The process is complicated by the fact that when an oxygen atom collides with an **(O_2)** molecule there is simply too much energy for them to combine. Hence a third **"minister" (M)** molecule is necessary to catalyze the union by removing the excess energy of collision (see Fig 3).

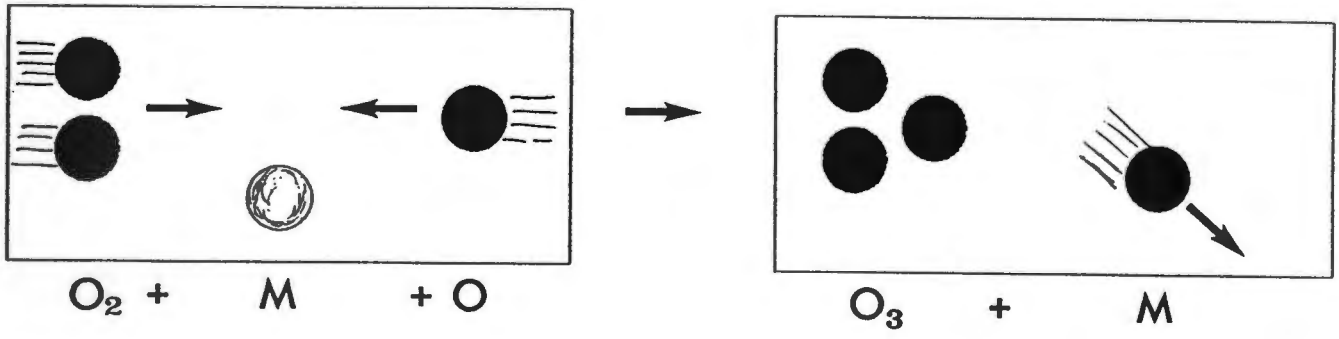

Before collision **After collision**

Figure 3. Formation of the ozone molecule in the upper atmosphere.

Presently the ozone layer is very much the subject of discussion and controversy. Only recently have scientists discovered that the quantity of stratospheric ozone is controlled by trace amounts of other substances whose concentrations are thousands of times smaller than that of ozone itself. Ozone is broken down by ultraviolet light but in the presence of pollutants such as chlorine and bromine the process is highly accelerated. The chlorine molecule in aerosol propellants **(Chlorofluormethanes or CMF's)** is liberated in the chemical process and has the ability to destroy thousands of ozone molecules. The bromine molecule has an even greater potential to destroy ozone.

In the upper atmosphere ultraviolet light breaks off a chlorine atom from a "chlorofluorcarbon" molecule. The chlorine atom then attacks the ozone molecule breaking it apart. An ordinary oxygen molecule and a molecule of chlorine monoxide are formed. A free oxygen atom breaks up the chlorine monoxide. This then leaves the chlorine free to repeat the process.

Perhaps the most dramatic effect of depleting the ozone layer would be to human health, where increased UV exposure could lead to a substantial increase in skin cancer. Another legitimate concern is that an increase in the UV-B radiation flux, due to ozone depletion, may lead to an increase in cataract incidence and other ultraviolet induced corneal diseases (Andley, 1987).

1.5. Objectives of the present study

The majority of ancient people worshipped the sun and viewed it as a health - bringing deity. During the eighteenth and nineteenth century therapeutic benefits of sunlight exposure were beginning to be understood and by the end of the nineteenth century the importance of ultraviolet radiation was being realized. Danish physician Niels Finsen, whom many regard as the father of ultraviolet phototherapy, also stressed that it was ultraviolet radiation in the solar spectrum which cause sunburn. We now recognize that the small portion of ultraviolet radiation which reaches the earth's surface is not necessarily therapeutic, but in fact could be harmful to humans. There are numerous accounts of the harmful effects of UV radiation to the skin and the eye as a whole. These effects may be caused by either acute or chronic exposure to UV radiation.

For example some acute effects of UV-B radiation include conjunctivitis and photokeratitis. "Snow blindness" and "arc welders eye" are further examples of acute ultraviolet damage specifically to the surface of the cornea. On the other hand chronic exposure to ultraviolet radiation is thought to be responsible for pterygia, climatic droplet keratopathy Hill and Maske (1989), cancers of the external eye, cataracts and various types of retinal diseases.

The present study is an extension of ongoing studies on ultraviolet radiation damage to the cornea in the Department of Ophthalmology, University of Cape Town and Groote Schuur Hospital. Their specific interest lies in the causes and

treatment of climatic droplet keratopathy. The aims of the present study are:

1) Establish a possible role of ultraviolet B radiation in human corneal diseases such as climatic droplet keratopathy and pterygium using the rabbit as an animal model.

2) Determine by means of SEM the initial effects and subsequent recovery of the epithelium after a 3 hour dose of ultraviolet B radiation. We refer to this study as "acute" response to ultraviolet B radiation.

3) To try and confirm the effects observed by SEM with ultrastructural studies using TEM.

4) In addition we are also looking at the possible effects after exposing rabbit cornea to a daily dose of low level ultraviolet B radiation, over a long period of time. We refer to this as chronic exposure to ultraviolet B radiation.

It is hoped that by exposing rabbits to ultraviolet light, principally ultraviolet B radiation, diseases similar to those found in humans could be simulated and disease progression studied. People are generally exposed to substantial amounts of UV radiation for a very long time. Since people generally live longer they will be exposed to an ever increasing amount of solar UV radiation and subsequently, there is an increasing risk of developing corneal diseases. The possible threat to the ozone is also a real possibility and could lead to increased levels of ultraviolet radiation reaching the earth's surface. This will require a greater understanding of the very nature of corneal damage due to acute and chronic exposure.

This study focusses mainly on the acute response to UV-B

radiation since most studies have investigated effects of prolonged exposure to UV light. Accordingly much less is known about acute exposure. Many people suffering from acute UV B radiation effects probably never visit the ophthalmologist or wait for a couple of days. This could also contribute to the fact that effects of short-term damage is not well documented.

LITERATURE REVIEW

2.1 Introduction

It was Widmark in 1889 who first reported that ultraviolet radiation caused a form of keratitis in the eye, commonly known at that time as photo-or UV-keratitis. Then in 1916 Verhoeff and Bell formulated some of the basic postulates relating to ocular damage caused by "ultraviolet radiation". In addition to conducting an experimental investigation of the pathological effects of radiant energy on the eye they also completed a systematic review of the literature at the time. In one of Verhoeff's experiments, he studied rabbit eyes using a quartz mercury lamp, which at that time produced 65% of the total radiant flux in the UV range. He reported that the abiotic effects of each exposure were additive within 24 hours; that is, the total cumulative exposure was responsible for the effects.

In 1929 Duke-Elder and Duke-Elder provided a summary of all the ocular photobiology cited up to 1929. In addition they conducted their own experiments where they studied the effects of exposing the rabbit cornea to an unfiltered medium-pressure

mercury quartz lamp. Histological sections from the sacrificed eyes were examined at various periods of time ranging from 2 hours to 10 days. It is difficult to compare their data with those of other researchers because of the broadband source of ultraviolet radiation in their experiments and because irradiance measurements were not reported. They do describe in detail the destructive and reparative processes that result from exposure to full-spectrum ultraviolet radiation (see Morphological changes). In addition they reported changes in the aqueous humour, iris, lens, and retina.

In 1945 Buschke observed changes in the mitotic activity of corneal epithelial cells following exposure to UV radiation. Buschke (1945) noted histologically that ultraviolet radiation was very destructive on the nucleus of the corneal epithelial cells and this same radiation had inhibitory effects on the healing process after exposure. These early studies on ultraviolet damage to the cornea relied on visual and light microscopic observations to categorize the damage, though they did establish important ground work for later more detailed studies using electron microscopy.

2.2 Electron microscopy of the corneal epithelial layer

The first ultrastructural studies on the rabbit corneal epithelial layer were carried by Aono (1961) and by Kaye and Papas (1962). Their transmission electron micrographs of the corneal epithelium showed numerous cytoplasmic protrusions (microvilli) and in two cases the micrographs revealed a complex

pattern of surface ridges or microplicae. The first scanning electron micrographs of the corneal epithelial surface were published by Blumcke and Morgenroth (1967). They were able to show that the microvilli and microplicae corresponded to the cytoplasmatic processes observed in the early transmission electron micrographs.

In 1973 Pfister published some excellent scanning electron micrographs of the corneal epithelial surfaces of several different animals, including the rabbit. The purpose of his study was to; a) resolve some of the anatomical inconsistencies seen by transmission microscopy showing only surface microvilli, with SEM micrographs which show both microvilli and full thickness holes of the corneal surface in a variety of animals, b) to describe how the tear film could remain stable in spite of the process of normal epithelial exfoliation. Pfister (1973) showed that previously published scanning electron micrographs of the corneal surface consistently revealed a heavy mucin coat which significantly obscured surface detail. He also noted that previous scanning electron micrographs of the corneal surface were recorded after the samples were either air or vacuum dried. At the time of his study it was known that the technique of air or vacuum drying produced severe surface distortions due to surface tension. Contrary to the hypothesis of Hoffman (1972) regarding the light, medium and dark cells, Pfister (1973) concluded that dark cells may be dark by virtue of the density or length of the microvilli, the presence of more adsorbed mucin, the nature of the plasma membrane, or a combination of factors. The reverse would be true of light cells. His study could only

characterize the nature of the cell surfaces but could not determine precisely the cause of lightness or darkness.

2.3. Morphological changes to the cornea from ultraviolet radiation

In 1972 Hoffman was the first to expose rabbit cornea to the collective spectrum of a mercury ultraviolet lamp and examine its effects on the cornea under the scanning electron microscope. Hoffman (1972) was interested to see whether the cell reaction to pathological impulses by ultraviolet irradiation could supply new aspects on the origin and function of those cells with different surface patterns. He hypothesized on the basis of his results that the different cells with various surface structures were transition stages of the same cell and for the time being the cells show only part of their surface, these being the small light cells with the greatest number of cytoplasmic processes. A later study by Ringvold (1983) focused on early morphological changes of the cell membrane after UV-radiation. Up to that time it was known that ultraviolet radiation caused a variety of biological effects depending on dose, wavelength tissue resistance and various other criteria. The changes due to ultraviolet radiation occurred after a time lag while the initial step or steps in the sequence of events taking place after UV-radiation were unknown. In these studies, the rabbit corneal epithelium was exposed to UV-radiation and the cornea was examined under the scanning electron microscope after exposure. He observed small plasma membrane defects after 30 minutes

exposure and suggested these defects may be the point where the initial damage begins.

Most studies had described the corneal epithelial response to UV radiation while much less attention had been directed toward the endothelial response to UV radiation. In 1984 Cullen *et al.*, studied the effects of ultraviolet-B radiation damage to the corneal endothelium in rabbits. He concluded that ultraviolet-B radiation does damage the corneal endothelium and that the endothelial damage response appears to be directly related to the exposure dose.

By 1985 a considerable amount of pathophysiologic information was available concerning different mechanisms impairing corneal hydration. On the other hand, details regarding UV-induced stromal changes were lacking. A study by Ringvold (1985) looked at the changes in the rabbit corneal stroma caused by UV-radiation. They reported that 3 days after irradiation there was epithelial loss and stromal oedema, which was most prominent in the anterior quarter of the stroma. Here many of the keratocytes were dead as a result of the radiation. In the remaining three quarters of the stroma, a large number of round or oval cells with nuclear fragmentation and abnormal inclusions were evident.

Apparently a detailed ultrastructural study of the rabbit corneal epithelial layer after exposure to UV-B radiation has not been performed. However, Pitts *et al.*, (1987) described the effects of 300 nm ultraviolet exposure on the primate cornea. Even less has been done with SEM. The only correlative TEM-SEM study found to date is by Hazlett *et al.*, (1980) who studied the

epithelial desquamation in the adult-mouse cornea.

2.4. The determination of ultraviolet threshold levels

Kinsey and Cogan (1946) examined the spectral transmission of the rabbit cornea to ultraviolet radiation and provided the first reliable quantitative threshold exposure data for spectral regions shorter than 320 nm. They used a mercury arc source and added a quartz prism monochromator to limit the spectral regions incident on the eye effectively using ultraviolet radiation in the 240 - 300 nm range. They found the radiant exposure threshold for corneal damage in the rabbit to be .015 Jcm^2 with a maximum sensitivity at 288 nm. At wavelengths longer than 313 nm they were unable to induce corneal damage, since the cornea absorbs wavelengths below 295 nm and transmits all longer wavelength radiation to the aqueous humour and the lens.

One problem with the mercury arc source is that it produces very strong emission lines at regular intervals in the ultraviolet spectrum. Due to these strong emission lines, exposures at equal wavelength intervals across the ultraviolet spectrum cannot be readily achieved. As a result, the number of points one selects along the waveband may not be adequate to sufficiently resolve the action spectrum. This problem was avoided by Pitts and Kay (1969) who used a high pressure Xenon-mercury lamp that provided a continuous spectrum from 200 to 500 nm. In their ultrastructural study they described increasing severity of damage to the epithelium at elevated levels of

energy. They used a grating monochromator to produce ultraviolet radiation with a 10 nm full waveband at 270 nm. Their results were able to establish the rabbit corneal threshold at 0.0156 Jcm^{-2}. They also established that the rabbit corneal action spectrum for photokeratitis ranges from 210 nm to 310 nm. They found that the most effective wavelength to produce photokeratitis was 270 nm, with an exposure dose of .005 Jcm^{2}. Cullen (1980b) also used a high pressure Xenon-mercury lamp and a double monochromator and determined the radiant exposure threshold in the rabbit to be 0.02 Jcm^{-2} at 295 nm. He found that the development of corneal epithelial granules were the most repeatable and reliable response for near threshold radiant exposures. The levels of irradiance used in Cullen's study were more accurately measured and controlled than in earlier work and the levels of radiant exposure were at or below a more critically defined threshold. In contrast, early investigators had difficulty in studying the mild abiotic response in the corneal epithelium due to problems of calibration and of reproducing levels of radiant exposure with accuracy.

2.5. Characterization of ultraviolet induced damage

Early morphological studies were based on light microscopic work and described cellular and nuclear degeneration, cell death, epithelial mitosis, and eosinophilic staining reactions. Detailed histological changes were reported by Duke-Elder and Duke-Elder (1929) who exposed rabbit cornea to a source of

ultraviolet radiation which contained UV-C, UV-B, UV-A and visible radiation. The excised corneas were studied at various periods of time ranging from 2 hours to 10 days.

The first signs of histological damage were noticed 4 hours after exposure, and consisted mainly of occasional swelling of a squamous or basal epithelial cell. The endothelium and stroma appeared normal. After a period of 6 hours, a large number of epithelial cell nuclei stained red, while the basal cells were widely spaced indicative of edema. As time increased they found these changes progressed and were most noticeable at 12 hours after exposure. They noticed that in some of the epithelial cells the entire nucleus was full of granules and usually surrounded by a vacuole-like space. Other observations through 12 to 24 hours included; swelling of the collagen fibres of the stroma, fragmentation of the keratocyte nuclei, abnormal staining of the endothelium similar to the epithelium, and desquamation in the central area of the cornea. They reported that few changes occurred between 24 and 36 hours after exposure. The epithelial cells then began to take on an orderly arrangement and the abnormal conditions gradually disappeared until in 7 days the cornea was essentially normal.

Duke-Elder and Duke-Elder (1929) also reported that after "mild" exposure to ultraviolet radiation, the abiotic changes which occurred stop, and the cells return to normal. They also noted that the traumatized cells recover rapidly and those that are killed or exfoliated are rapidly replaced by fresh cells.

Pitts and Kay (1969) established a corneal action spectrum for the rabbit used the following criteria to describe corneal

damage; epithelial debris, epithelial stippling, epithelial granules, stromal haze, stromal opacities and endothelial disturbances. Pitts (1977) qualified the criteria as follows: epithelial debris is described as small, glistening bodies located in the precorneal tear layer, epithelial haze as an irregular crackled appearance of the corneal anterior surface, epithelial granules as small, discrete round white spots located deep in the epithelial layer, epithelial exfoliation as a sloughing of layers of the epithelium, stromal haze as a loss in the transparency of the stroma, stromal opacities as local areas of opacification and endothelial disturbances as granular formations similar to epithelial granules.

A later study by Cullen *et al.*, (1984) who also used pigmented rabbits, correlated the biomicroscopic picture with that observed by the electron microscope. They found that the first clinical signs of trauma as observed with the slit-lamp microscope were granules which occurred after radiant exposures of 0.05 Jcm^{-2} or greater. At the EM level, they found giant lysosomes which they determined corresponded to the observed granules; however, small lysosomes were present at the EM level after the eye was exposed to only 0.014 Jcm^{-2}. This led Cullen *et al.*, (1984) to conclude that the EM was approximately 4 times more sensitive than a biomicroscope in determining threshold values.

Ringvold (1983) used scanning electron microscopy (SEM) to observe the following morphological changes to the surface of the rabbit corneal epithelium after UV-radiation: 1) A reduced number of the large impressions or full-thickness holes on the

superficial cells. 2) An increased number of partly rejected cells. 3) Numerous small plasma membrane defects. He concluded that the UV-radiation caused biochemical changes which rapidly led to cell rejection. The small plasma membrane defects only appeared after approximately 60 minutes of irradiation. He also noted that these same small membrane defects were lacking in the cornea irradiated through window glass, which roughly excludes wavelengths below 350 nm.

No detailed correlative SEM-TEM study of the rabbit cornea subjected to both acute and chronic levels of ultraviolet B radiation has been found in the literature. This study was undertaken to better understand and characterize corneal epithelial damage following acute and chronic exposure to the ultraviolet B waveband. Following these early studies, many aspects of corneal damage following ultraviolet radiation and threshold values are now well established and accurate. The subject of corneal damage after UV-irradiation has by no means been exhausted and hopefully this study will compliment that which has already been discovered.

THE CORNEA

3.1. The cornea: basic structure and function

The cornea forms part of the tough outer tunic of the eye and is a major component in the optical system of the eye. The cornea withstands the intraocular pressure from within and

protects the inner contents from mechanical injury from without. The cornea is essentially a transparent, flexible membrane of high tensile strength, inflated by internal pressure. This strength is due to the presence and arrangement of the collagen fibrils making up the lamellae within the corneal stroma.

The cornea has a similar optical function to the lens, that is it must be transparent to visible light and it must be capable of refracting the central core of incoming light so that it focuses on the appropriate region of the retina. The cornea has approximately two thirds of the eye's refractive power and to this end it is curved and transparent. Its surfaces, particularly the external one, are smooth to good optical standards. Although the cornea has a fixed focus, in combination with the lens which is capable of altering its focusing power, a sharp image is formed on the retina of the emmetropic eye.

The cornea's optical properties are determined by; its refractive index, its transparency to visible light and by its radius of curvature. The refractive index in turn is determined by the cornea's chemical composition while its transparency to visible light is dependent on avascularity, morphology and chemical composition. Finally the radius of curvature is determined by growth and development of a normal cornea. The cornea most resembles a watchglass, its curvature varying among species. In man, and to a lesser extent in many other species, the cornea is more curved than the eyeball as a whole. It is slightly elliptical on its outer surface, with the longer axis horizontal. In the human for instance, its thickness ranges from 0.50 to 0.57 mm in the centre to about 0.66 to 0.67 mm at the

periphery. In the rabbit the thickness is approximately 0.40 mm.

The physical basis of corneal transparency is based on the lattice arrangement of the collagen fibrils. The density of light scattering particles is the same throughout the tissue, therefore, the total intensity of scattered light will be zero. Accordingly the cornea is perfectly transparent if the density of scattered particles is uniform throughout. It is obvious from this physical basis of corneal transparency that any disturbance of this arrangement will lead to corneal opacification. Any form of edema would disturb this regular arrangement of the collagen fibrils resulting in a cloudy cornea. Thus corneal transparency is extremely sensitive to its state of hydration. This is where the epithelium and endothelium play a major role in the metabolic maintenance of the cornea by an active as well as a passive process.

The structure of the cornea can be divided into 5 distinct layers lying parallel to its surfaces, three of which are cellular. From without inwards they are: the epithelium + tear film, Bowman's membrane, the stroma (substantia propria), Descemet's membrane and the endothelium.

3.1.1.The tear film

The cornea itself is covered by a thin liquid layer known as the tear film which is approximately 7 μm, thick including the mucous layer on the surface of the cornea. The tear film minus the mucus layer consists of a thin lipid film (~0.1 μm) floating on a large aqueous lake (~7.0 μm).

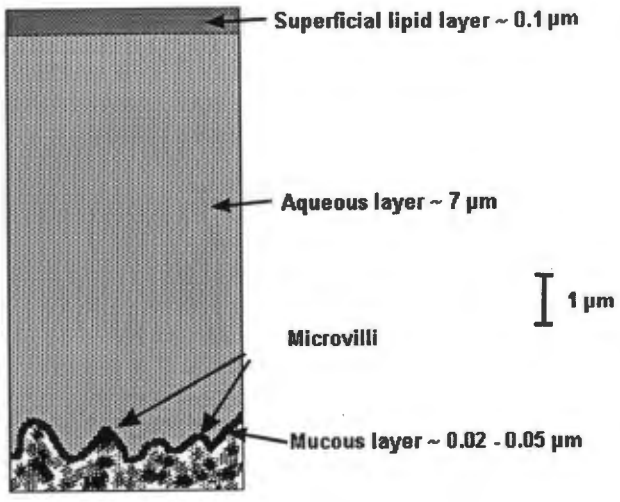

Figure 4. The three layers of the tear film drawn to scale from Holly and Lemp (1977).

The tear film performs several important functions in the eye: 1) Forms and maintains a smooth refracting surface over the cornea, 2) Maintains a moist environment for the epithelial cells of the cornea and conjunctiva, 3) Has bactericidal properties, 4) Transports metabolic products, 5) Provides a pathway for white blood cells in case of injury.

The outer lipid layer behaves as a film essentially independent of the aqueous layer underneath. It is there primarily to inhibit evaporation of the tears, more so under conditions of low humidity and turbulent air flow. The underlying aqueous layer makes up the bulk of the tear film and acts as the major metabolic pathway for the corneal epithelial cells. It is here where the numerous solutes, electrolytes, proteins and other tear components are found. The mucous layer which directly covers the epithelial cells is very hydrophillic and coats the entire epithelial surface, thus rendering it wettable by the aqueous tears.

3.1.2. The epithelium and basement membrane

The epithelial surface of the cornea consists of nonkeratinized, squamous cells of five to seven layers. It is the most regularly arranged of all squamous epithelia in the body and makes up about approximately 10% of the total corneal thickness in the rabbit cornea.

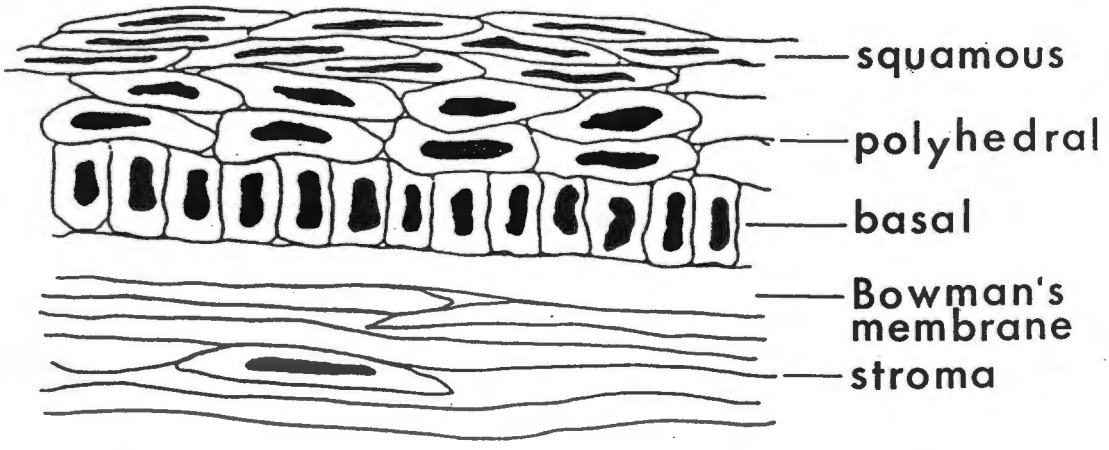

Figure 5. Transverse section of the normal corneal epithelium, reproduced from Zuclich (1984).

The innermost basal layer is composed of single layer of densely packed columnar cells. Daughter cells of this basal layer are forced outwards to form the two or three intermediate layers. The basal cells have extremely interdigitating cell membranes, sometimes called intercellular bridges and are attached to the underlying basement membrane by numerous hemidesmosomes. Along with anchoring fibrils, these attachment complexes are responsible for a tight adhesion of the epithelium to the underlying Bowman's layer. A thin uniform basement membrane which is secreted by and closely applied to the under surface of the

basal cells is also part of this anchoring structure.

The middle layers of the epithelium are composed of polyhedral epithelial cells which become increasingly flatter as they migrate towards the superficial layer. They may reach as much as 40 μm in length and are about 4 μm in thickness as they approach the superficial layer.

The superficial layer consists of extremely attenuated overlapping squamous cells approximately 45 μm long and flat. The nuclei of these cells become flattened as they move towards the surface, since in the basal layer the nuclei are almost spherical (Davson, 1980). The outermost surfaces of these cells are in contact with the tear film and are covered with microvilli and microplicae, some of the microvilli are up to 1 μm in length and occur in a random reticular or corrugated pattern. These microprojections greatly augment the free surface area, thus increasing tear film retention as well as enhancing diffusion and active transport processes.

The corneal epithelium's function is to provide a very smooth refractive surface at the front of the eye. It is relatively impermeable to water soluble agents from the tear film and to bacterial and fungal infections. It also helps to maintain proper corneal hydration by reducing evaporation and minimizing absorption of fluid from the tears. The main substrates for energy production are glucose and glycogen which primarily comes from the aqueous humour. The epithelium also has large glycogen stores available in response to those metabolic demands that cannot be met by free glucose, as in the case of mild trauma.

3.1.3. The stroma and Bowman's layer

Bowman's layer is situated immediately subadjacent to the epithelium and basement membrane. Although lacking in the rabbit, its structure is still important and should be detailed. Its an area approximately 10 μm thick, cell free and consists of randomly orientated collagen fibrils of relatively small diameter embedded within a glycosaminoglycan ground substance. The fibrils are similar to those found in the stroma but only about two-thirds of their diameter. It is most distinctive in man and the primates while in most other mammals it is very thin and only suggested as a condensation of the stromal surface.

The two primary properties of the outer tunic of the eye - transparency and mechanical strength - are both met by the stroma. The stroma makes up about 90% of the thickness of the cornea in the rabbit and most other mammals. It consists of regularly arranged sheets of collagenous material lying parallel to the surface, known as stromal lamellae. The fibrous nature of the lamellae are evident when teased out and *in situ* pursue a wavy course relative to the surface of the epithelium. There are 200 to 250 stromal lamellae, each about 2 μm thick. The collagen fibres within the lamellae have a circular section and uniform diameter (30 nm in the rabbit, +/- 0.5 nm (Giraud *et al.*, 1975) and run parallel to each other in layers. Isolated fibres, when separated with the minimum of preparation, are found to be coated with a sheath of amorphous material. The uniform diameter of the collagen fibrils, their parallelism within the layers, the

relatively equal distances among them, and the even layering of the arrayed lamellae contributes to the transparency of the cornea.

The main cellular constituent of the stroma is a modified fibroblast known as a keratocyte. Under normal conditions keratocytes are relatively few, accounting for only 5 percent of the corneal dry weight. These cells are found at all levels of the stroma and generally lie between the lamellae. Their organelles are typical of a protein-secreting cell; free ribosomes, rough endoplasmic reticulum, golgi apparatus, lysosomes, secretory vesicles and mitochondria. The keratocytes are able to produce the collagen and matrix of the stroma, actively participate in wound healing and are also involved in other pathologic processes (Smolin and Thoft, 1983).

3.1.4. The endothelium and Descemet's membrane

Descemet's membrane is a true basement membrane which is derived directly from the endothelial cells and lies between the stroma and endothelium. In the normal human adult it may attain 10 to 15 μm in thickness and biochemical characterization indicates that it is constructed of collagen. Descemet's membrane is able by itself to bear the intraocular pressure in pathological conditions where the stroma is dissolved away. It appears to be the most resistant layer of the cornea to chemical, bacteriological or autolytic activity (Cogan, 1951).

The endothelium is a single layer of cuboidal cells lining the inner surface of the cornea. These cells form a very

distinctive hexagonal mosaic, contain a large nucleus, abundant mitochondria and have a well developed system of rough endoplasmic reticulum and golgi bodies. The lateral plasma membranes of adjacent cells are extensively interdigitated, thus forming a continuous monolayer of closely apposed cells. This tightly packed monolayer is suited for its function as a barrier to fluid flow and as an actively transporting ion pump. The endothelium acts against forces that tend to draw or force water into the corneal stroma. This is critical, as major increases in hydration can cause a loss of transparency and even slight changes in hydration can cause some slight clouding of the cornea (Maurice, 1957).

3.2. Optical properties of the cornea and response to UV radiation

The outer surface of the cornea must be smooth to within 0.3 μm in order to account for the optical resolution of the eye (Davson, 1990). From the previous discussion on the morphology and composition of the cornea it has been demonstrated that the cornea should be transparent to and transmit all visible light (400 to 750 nm). This transparency, as mentioned earlier, is highly dependent on the hydration of the corneal tissue. Apart from absorbing some of the incident light that falls on it, the stroma also scatters a small portion. This light scattering of the stroma rises rapidly as the tissue swells and transmittance at any wavelength was found to decrease linearly with increase in stromal thickness (Farrell *et al.*, 1973).

The maximum of the eye's spectral response corresponds roughly to the maximum of solar spectral irradiance and because solar ultraviolet radiation is present during most of the daylight hours, the eye may be exposed daily to some amount of solar ultraviolet radiation throughout life. When considering ultraviolet transmission and absorption, the type and extent of damage to ocular tissue depends on the energy absorbed, the wavelength of the radiation, and the duration of the exposure. The ocular tissues affected by UV exposures are generally those in which the radiation is absorbed. Ultraviolet transmission data published by Kinsey (1948) demonstrates that soft X-rays and ultraviolet radiation below 310 nm (UV-B and UV-C) is absorbed principally by the cornea and the biologic effects of these wavelengths are seen predominantly in the corneal tissue. UV-A radiation is absorbed by the cornea and the lens. The cornea is made up of 75% water, approximately 20% protein, approximately 1% polysaccarides, lipids and nucleic acids Lerman (1984). Over 99% of the cornea's chemical composition is made up of molecules that contain chromophores absorbing only in the UV regions between 200 and 295 nm. The water and carbohydrate molecules will absorb UV radiation below 230 to 235 nm, nucleic acids absorb at approximately 250 to 260 nm, and the protein component in the 235 to 250 nm region (aliphatic amino acids) and in the 270 to 295 nm region (aromatic amino acids) Lerman (1984). In the ground substance of the corneal stroma, the protein portion is responsible for absorption of the UV radiation in the 275 to 295 nm region.

Unlike the skin, the ocular system does not develop a

tolerance to repeated ultraviolet exposure as the tissues do not contain melanocytes. In the skin, melanin production by melanocytes is induced following UV exposure. The melanin, in conjunction with an increase in skin thickness, then decreases the amount of UV radiation penetrating the dermis (Coohill, 1987).

3.3. Ultraviolet induced corneal diseases

Historically ultraviolet damage to the cornea was first studied qualitatively by Voerhoeff and Bell (1916). Interestingly, they were the first to point out that this UV induced damage was both wavelength and intensity dependent. Subsequently Duke-Elder and Duke-Elder (1929) were the first to define "Pterygium", a disease in which the chronic exposure to ultraviolet radiation has been implicated.

We can say that the cornea is to some extent resistant to natural ultraviolet induced damage. Steady exposure to a combination of sun, sky and reflective natural surfaces in a temperate climate should cause photokeratitis in approximately 10 minutes, yet this does not happen. This resistance to average levels of ultraviolet radiation can be predicted from results of a number of animal studies (Voerhoeff and Bell, 1916; Kinsey, 1948; Pitts, 1977).

On the other hand, we know that the cornea can be damaged by excessive shortwave ultraviolet radiation, such as that produced by man-made sunlamps and arc welding beams. These man-made sources cause an acute form of "keratitis". One must also

take into account that there are extreme natural conditions, such as the highly reflective nature of snow, ice and desert sand which cause a form of keratitis known also as Labrador Keratitis.

3.3.1. Ultraviolet induced keratitis - acute damage

Since the initial work of Voerhoeff and Bell (1916) , the effect of wavelength dependence on acute damage to the cornea has been thoroughly explored, Kinsey (1948) Pitts (1977). The most range of wavelengths that produce the most corneal damage are those between 260 - 290 nm, Pitts (1977). If we now focus on the relationship between wavelength and threshold energy needed to produce a corneal lesion, then at about 270 nm, only 0.005 J/cm^2 of energy will produce a lesion, at 300 nm about 0.01 J/cm^2 and at 320 nm approximately 10 J/cm^2. At 320 nm to produce a lesion requires about 2000 times the energy above the lowest threshold. From this data we can see that an incredibly small amount of short wavelength UV light can cause corneal damage.

The short wavelength UV radiation that we experience on earth comes from man-made sources. A form of ultraviolet induced "keratitis", ie. actinic keratitis would occur in nature after prolonged UV exposure as in the case of "snow-blindness".

The nucleic acids found in the epithelium and endothelium absorb maximally at these shorter wavelengths, in addition certain aromatic amino acids also absorb these shorter wavelengths. Histologically, damage from this absorption includes epithelial cell swelling, death, and desquamation associated with

keratocyte changes, stromal swelling, endothelial damage and an anterior uveitis.

3.3.2. Climatic droplet keratopathy

First described clinically in 1965 by Freedman , "climatic droplet keratopathy" (CDK) has been given a variety of other names including; Labrador keratopathy, spheroidal degeneration, chronic actinic keratopathy etc. Initially attributed to chronic exposure to UV radiation in an Arctic environment (Freedman, 1965; Norm, 1984), this condition is also particularly common in rural areas of South Africa and many other Third World countries.

The exact cause of climatic droplet keratopathy is unknown, but certain factors such as; solar radiation, aging, low humidity, microtrauma from wind, sand and ice and possibly extremes of temperature and previous corneal inflammation seem to be related to its progress (Freedman, 1965). Climatic droplet keratopathy most often affects men who work outdoors.

Climatic droplet keratopathy appears as a corneal haze which histologically shows up as tiny droplets beneath the epithelium and in the superficial corneal stroma (Miller, 1987). Electron microscopy shows the globules to be markedly electron-dense with little or no structure. Four grades of severity have been described; 1) Limbal areas of the cornea only. 2) The opacity spreads to the pupillary area but with vision normal. 3) As in (2) but vision is significantly impaired. 4) Large, yellowish, opalescent nodules elevate the epithelium. There is no known

cure, and once vision is severely impaired a corneal graft must be considered.

3.3.3. Pterygium

Although this disease has been defined since 1954 by Duke-Elder, there is still much controversy concerning the aetiology and pathogenesis of pterygium. Chronic exposure to ultraviolet radiation appears to play an important role in the pathogenesis of this disorder, although evidence for this is primarily epidemiologic (Hill and Maske, 1989). A direct causal relationship between UV radiation and pterygium has not been proved, and there is conflicting evidence indicating that chronic inflammation from other causes can induce the disease (Hill and Maske, 1989). It is interesting to note that on a world distribution basis, Cameron (1965) found that countries that are hot, dry and dusty have a higher prevalence of pterygium. But there were other areas that, although hot, were neither dry nor dusty and yet also had a high prevalence of pterygium. It seems that a common factor here is latitude, the disorder occurring mostly between the latitudes of 37 north and south of the equator. Interestingly, ultraviolet radiation also varies with latitude and this fact is what Cameron (1965) considered important in the aetiology of pterygium.

Histologically, pterygia are fibrovascular connective tissue overgrowths of the bulbar conjunctiva onto the cornea (Grayson, 1979).

MATERIALS AND METHODS

4.1. Sources of ultraviolet radiation

Ultraviolet radiation can be produced artificially by heating a body to an incandescent temperature or by the excitation of a gas discharge. The most common artificial sources are; mercury discharge lamps with or without a fluorescent coating, mercury vapour arcs operating at various pressures, metal halide lamps and the xenon arc lamp. In addition, lasers have been developed recently which emit intense, coherent beams of monochromatic ultraviolet radiation, although the availability and prohibitive cost has limited their use in research applications.

The characteristics of a radiation source are defined by its spectral distribution, or the more commonly used but somewhat inexact term, "the emission spectrum". The emission spectrum describes the range of wavelengths and also the relative amounts of each wavelength emitted by the source in question.

We initially planned to use a high pressure mercury vapour lamp as our artificial source of ultraviolet radiation. With the aid of a monochromator and specific optical filters we would be able to precisely select a specific portion of the UV-B radiation band for our experiments. Obtaining the specific optical filters and a working monochromator proved to be both costly and strewn with problems. In addition there are three important practical considerations in the use of filters; 1) the transmittance of a filter is a curve, and thus the cutoff has a slope and is not vertical, 2) filters invariably eliminate a proportion of the

desired wavelengths, 3) filters often age or "solarize" owing to photochemical alterations induced by the incident radiation and these alterations change the transmission of the filter and hence the emission spectrum of the filtered radiation source.

As an alternative we decided to use specific fluorescent "sunlamps" which according to the manufacturers produce over 50% of their total radiation in the UV-B range. The fluorescent lamp is basically a highly efficient conversion device which transforms ultraviolet energy into light or a specific band of ultraviolet radiation. The lamp operates when a discharge through a low pressure of mercury vapour occurs within the lamp. The mercury vapour is an efficient ultraviolet generator. The ultraviolet radiation so produced is absorbed by the phosphor coating on the inside of the glass wall. The phosphor fluoresces and reradiates the absorbed energy as longer-wavelength visible energy. The composition of the phosphor in a particular lamp determines which wavelengths are re-emitted and is a trade secret, but essentially these phosphors consist of mixtures of silicates, borates and phosphates of alkaline earth metals.

For our experiments we decided to use fluorescent sunlamps, which in the past have been used extensively in UV-B phototherapy though they have not been used previously to study ultraviolet radiation damage to the rabbit cornea. The type of fluorescent sunlamps we required are produced by Philips and Sylvania. There is however a marked difference in the spectral output between the Philips and Sylvania lamps (see Fig.6). The spectral distributions of these two different fluorescent sunlamps are detailed in Table I.

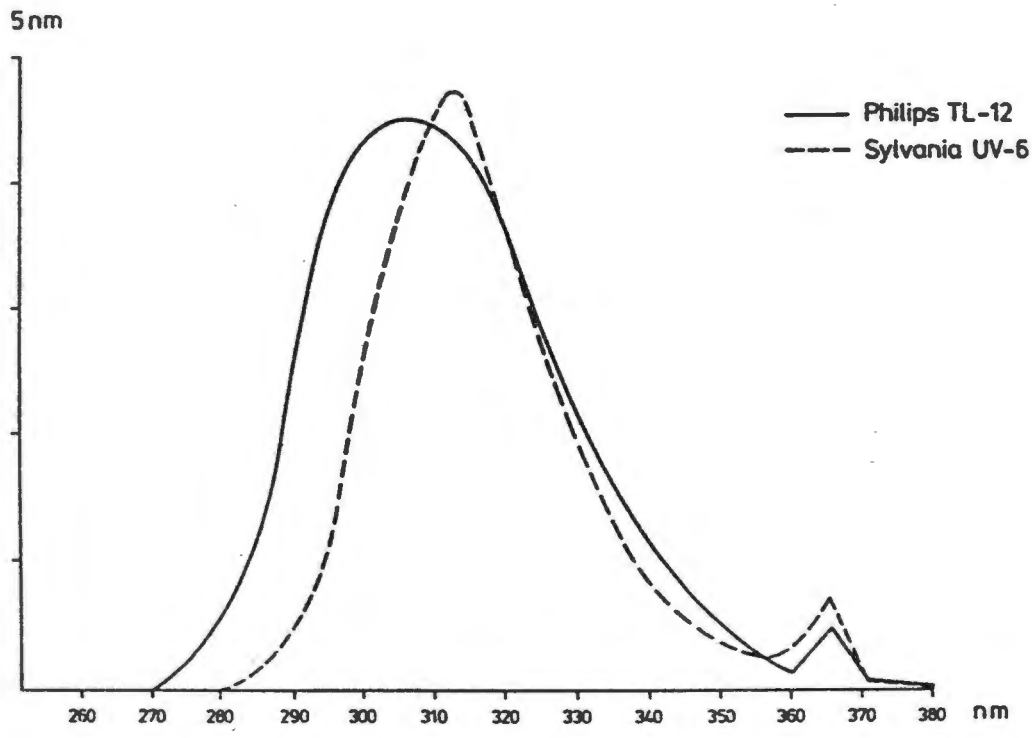

Figure 6. The emission spectra of two fluorescent sunlamps; Sylvania F 75/85W UV-6 and Philips TL-12. Spectral distributions provided by Philips Nederland B.V., Eindhoven (The Netherlands) and Waldmann GmbH, Schwenningen (W. Germany).

If we look at Fig. 6, we can see that the Sylvania lamp exhibits a spectral shift toward the longer wavelengths, which is apparent when one compares the spectrum distributions of the two lamps (Table I).

TABLE I.Spectral distribution vs wavelength of the Philips TL-12 and Sylvania UV-6 fluorescent sunlamps.

	<280nm	280-320nm	320-400nm	>400nm
Philips TL 12	**0.4%**	**62%**	**32%**	**5.6%**
Sylvania UV 6	**0%**	**51%**	**31%**	**18%**

The Philips lamps emit a higher percentage of UV-B

radiation, an important consideration for our work. Since the Philips lamps produce 11% more UV-B radiation than the Sylvania lamps we settled on the Philips TL 12 lamps. Fortunately we were able to secure 3 Philips TL 40 W/12 from the Dermatology department at Groote Schuur Hospital. These second hand lamps which had been used for a short period of time, actually provided an advantage since fluorescent lamps suffer from erratic and rapid aging during the first 12 hours or more of operation. We measured the output of the lamps by placing a radiometer at the same position as the experimental rabbits.

4.2. Ethical considerations

The use of rabbit eyes for experimental purposes is a sensitive and emotive one hence due consideration and care must be taken for the animals during all phases of the experiment.

This research project was conducted in part to obtain an animal model with which to investigate various aspects of corneal disease in humans, specifically those diseases attributed directly to exposure to ultraviolet radiation. Since the experiments would subject the rabbits to acute levels of ultraviolet radiation, thereby inducing a form of keratitis, permission for this work was obtained from the Ethical Committee of the Medical School at the University of Cape Town (No 89/30).

The animals were sacrificed by the animal technician in charge who used a lethal dose of Sagatol (pento barbitone sodium). Once the animals were pronounced clinically dead, the corneas were surgically removed and processed for electron

microscopy. Surgical removal of the cornea was performed by a qualified Ophthalmologist.

4.3. Experimental protocol

We designed an experimental setup to examine the acute phase experiments by placing the rabbit in a specially designed retaining box such that the rabbit's head was exposed and maintained in a stationary position. The restraining box containing the rabbit was then placed on the floor so that the exposed eye would be perpendicular to the light source (see Figure 7). Since the terminal 6-12 inches of a fluorescent lamp has a much lower output than the centre, it was important to place the rabbit centrally in relation to the bank of fluorescent lamps. We used both male and female pigmented rabbits for the experiments.

At the beginning and end of the 3 hour exposure period the rabbits all had their eyes open and did not show any excessive blinking. We did not use a speculum because it would dry the eyes, hence we had no way of knowing when the rabbits actually blinked during the experiment or if their eyes were closed for any length of time. To monitor such an event would have required elaborate and expensive equipment, something we simply couldn't afford.

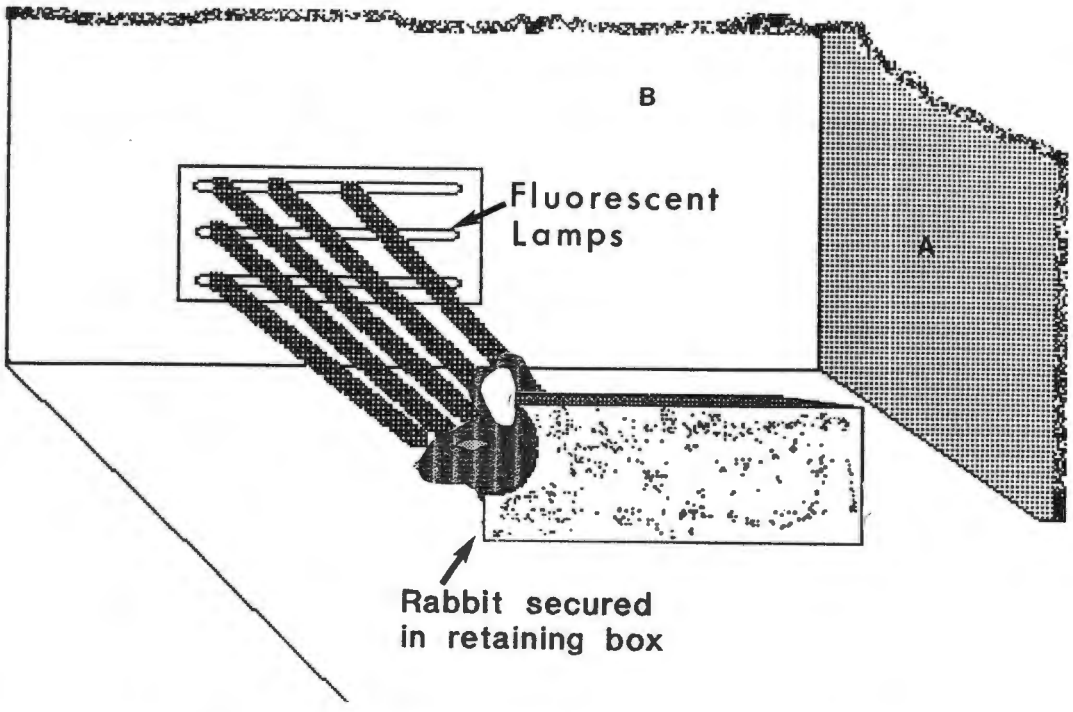

Figure 7. Schematic drawing of our experimental setup showing the rabbit, restraining box and position in relation to the fluorescent lamps. Panels A and B are part of the painted styrofoam enclosure.

For the **"acute"** exposure phase of the experiments the rabbits were placed on the floor at a distance of 1 meter from the bank of fluorescent lamps and exposed for 3 hours using all three lamps. This exposure dose of 0.31 Jcm^{-2} was sufficient to produce keratitis in the cornea. Keratitis was diagnosed by means of a slit lamp optical microscope and presence of a deep red colour within the cornea was used as a clinical indication of keratitis. The rabbits and the fluorescent sunlamps were surrounded by an enclosure made of sheets of styrofoam painted matt black on the side facing the rabbits. This was done to eliminate any possibility of reflection from the walls, floor or ceiling of the room. Internal reflection could influence the actual radiation dose of the exposed eye. The rabbits used in our experiments and the exposure\recovery schedules are listed in Table II and Table III.

Table II. Acute Exposure. Clinical record showing the exposure/recovery schedule of the acute phase of the experiment.

Rabbit number	Date exposed	Side	Length of exposure	Recovery prior to removal
178	Sept 15/87	right	3 hours	none
272	Apr 29/88	left	3 hours	3 hours
196	Feb 2/88	right	3 hours	16 hours
242	Nov 10/87	left	3 hours	24 hours

Table III. Chronic exposure. Clinical record showing the exposure schedule of the chronic phase of the experiment.

Rabbit number	Date exposure started	Side	Daily dosage	Date cornea removed
196	Oct 9/87	left	1 tube, 1 hr at 2 metres	Feb 5/88
196	Jan 23/88	left	1 tube, 2 hrs at 2 metres	Feb 5/88
240	Feb 1/88	left	1 tube, 2 hrs at 2 metres	Jun 24/88

In these experiments the "acute" exposure refers to a dose of radiation strong enough to induce keratitis while the "chronic" exposure dose was sufficiently low enough so that no signs of damage could be detected with the optical slit lamp microscope. The "recovery" period refers to the time frame between switching off the lamps and sacrificing the rabbit. The measured radiation doses used in this study are listed in TABLE IV, on page 51.

In the "Chronic" exposure schedule, rabbit 196 was initially exposed to only 1 lamp for 1 hour per day at a distance of 2 meters from the lamp. After 107 days of a daily 1 hour exposure there were no visible clinical signs in the cornea. It was decided to increase the daily dosage from January 23 to 2 hours per day, lamp and distance parameters remaining the same. This dosage was still below the level which is known to induce keratitis.

4.4 Control Corneas

In order to recognize and identify any early morphological changes at the EM level attributable to ultraviolet radiation, it was necessary to obtain a control unexposed cornea processed identically to the irradiated cornea. We sacrificed a pigmented rabbit from the same group of animals which had not as yet been exposured to our fluorescent lamps.

4.5. Preparation of the corneas

The entire cornea with a 1mm rim of sclera was surgically removed by a registered ophthalmologist from the Department of Ophthalmology and placed epithelial side down in a dry silicone cup. It was not practical to process the entire cornea for SEM as the outer sclera being fibrous in nature causes the cornea to curl up excessively after being critical point dried. To overcome this problem we used a 6 mm trephine to remove a 6 mm corneal button from the central area of the excised corneas. After the first two corneas were processed and critical point dried it was found that the 6 mm button still curled up excessively. To overcome this problem we decided to use a smaller 4 mm trephine for the remaining corneas. The 4 mm corneal disc curled only slightly during processing and was much easier to mount on the SEM stub. This procedure also allowed us to trephine two 4 mm buttons from a single cornea, one for scanning microscopy and one for transmission microscopy.

Within the limits of this study it was not possible to compare ultraviolet damage from different areas of the cornea. Our main interest was to determine the changes occurring predominantly in the important central area of the cornea.

4.6. Processing of tissue for scanning electron microscopy

The corneal buttons were immediately placed in a vial of cold buffered glutaraldehyde and processed according to the

following schedule:

Fixation: 2.5% glutaraldehyde made up in 0.2M Sorensen's phosphate buffer at 4°C, pH 7.2 with 6.15 g sucrose added per 100 ml.

Washing: wash with several changes of 0.2M phosphate buffer, pH 7.2.

Post-fix: in 1% buffered osmium tetroxide, fix for 1 hour.

Washing: wash in several changes of 0.2M phosphate buffer.

Dehydration: through a graded series of ethanol; 50% 70% 90% 95% - 2 times 10 min in each grade of ethanol.

After dehydration in 95% ethanol the samples were passed through several changes of molecular sieve dried 100% ethanol to remove all traces of water. The samples were then critical point dried in a Polaron E3000 Critical Point Drier (CPD) over a period of 3 hours using liquid carbon dioxide as the transitional fluid. Upon removal from the CPD the samples were immediately placed in a dessicator to prevent any rehydration. The corneas were then mounted on Cambridge 1 cm diameter aluminium stubs using a mixture of colloidal graphite and ordinary white glue as the adhesive. The samples were sputter coated with a layer of gold palladium alloy (60/40) in a Polaron E5100 series II cool sputter coater using argon as the ionizing gas. The samples were coated for a total period of 2 minutes at 2.0 kV and 12 mAmps current. The two minute coating time was pulsed at 30 seconds on, 5 second off to allow any heat to dissipate. The Series II cool sputter coater incorporates a sputtering head of a design in which the

gold/palladium target is surrounded by a cylindrical chamber fitted with a shaped magnet, the effect of which is to enhance sputtering rates but more importantly limit heating of the specimen surface due to electron bombardment. The stage holding the stubs is electrically cooled to channel away as much heat as possible. This was an important consideration due to the delicate nature of the corneal epithelial cells. We wanted to insure that any surface damage was due to the ultraviolet radiation treatment and not due to any excessive heating or electron bombardment from the sputter coater.

Micrographs of the epithelial surface were recorded with a Cambridge S200 scanning electron microscope. The instrument's operating parameters were set to 15kV accelerating voltage, specimen tilt at 30 degrees, a working distance of 11 mm and a final aperture of 100 microns. These conditons were chosen to yield good resolution at higher magnifications, good surface detail and minimum specimen damage from electron bombardment. Micrographs were recorded on Ilford FP4 120 roll film and developed in Rodinol 1 shot developer for 4 minutes at 20 °C. The micrographs were printed up on Ilfospeed multigrade RC paper.

4.6.1. Processing of tissue for transmission electron microscopy

The corneal button for transmission electron microscopy was processed identically to the one used for scanning microscopy up to and including the step where the sample is dehydrated through several changes of 100% ethanol. At this stage the samples were

further processed as follows:

Dehydration 100% ethanol, several changes, 100% propylene oxide, 2 times 10 min. The samples were then placed in a 1:1 mixture of propylene oxide and embedding media and infiltrated on a rotating device for 1 hour.

There are several embedding mixtures available for animal tissues, however we chose to use a mixture of Epon/Araldite according to the recipe formulated by Mollenhauer (1964) because it gave consistently good results in our laboratory. This mixture was originally used for plant tissues but has since proven to be popular for a wide range of tissues. The mixture was easier to section than one containing Epon alone. Tissue preservation was as good.

	Volume	Weight equivalent per 10 ml	Grams used
Epon 812	**25 ml**	**12.4 g**	**31.0 g**
Araldite 502	**15 ml**	**11.1 g**	**16.6 g**
DDSA	**55 ml**	**10.0 g**	**55.5 g**
DMP-30	**1.5%**	**1.0 g**	**1.5 g**

Following infiltration in the 1:1 mixture of propylene oxide and embedding mixture the samples were transferred to 100% fresh embedding media and infiltrated overnight on a rotating device. The following day the sample pieces were removed and placed in

flat embedding moulds, labelled and fresh embedding media was added. The blocks were polymerized at 60 °C for 48 hours.

Ultra thin sections were cut with a Reichert OM-U2 ultramicrotome fitted with a Dupont diamond knife. The resultant silver and gold sections (60 to 90 nm thick) were picked up on uncoated 200 or 300 mesh copper grids. In order to impart sufficient contrast the sections were stained with saturated aqueous uranyl acetate, 30 to 40 minutes followed by Reynolds lead citrate, 8 to 10 minutes. The sections were then ready for viewing in the transmission electron microscope. The sections were examined in a JEOL 1200 EXII transmission electron microscope set at an accelerating voltage of 80 kV. Micrographs were recorded on Ilford EM sheet film (3" x 4") at an exposure of 2 seconds. The smallest objective aperture was used for maximum contrast. Micrographs were printed on Ilford Ilfospeed multicontrast paper using a Durst LABORATOR 138 S enlarger fitted with an opal bulb as the illumination source.

4.7. Ultraviolet source measurement: Introduction

Radiation sources such as fluorescent lamps differ widely in their spectral output, purity and power yet several distinct advantages make them the most frequently used source of non-ionizing radiation. Fluorescent lamps do have some disadvantages which have practical implications; for example they exhibit erratic and rapid aging during the first 12 hours or more of operation and have a variable output during the first few minutes

of operation. Other factors which can affect their radiant intensity is operation at a high temperature, for instance, with inadequate ventilation. Since the lamps were second hand and the room in which the rabbits were being irradiated had adequate ventilation these limitations were not a factor in our experiments. Due to problems in obtaining a suitable radiometer, the lights were only calibrated at the end of the experiments. The values recorded are therefore "once off" readings. The advantages of low cost, reliability and the capacity to irradiate large areas with a reasonable uniformity of intensity made these lamps the prime choice for our experiments.

4.7.1. Instrumentation

In order to quantify the source of radiation and to see that the lamps were operating properly it was necessary to accurately measure their output of ultraviolet B radiation. This measurement was crucial for the chronic phase of the experiment as we had to be sure the dose would not cause keratitis.

The experimental level of irradiance is usually measured with a direct measuring instrument, called a "radiometer". A radiometer is simply a device used to measure the irradiance of a source of photons. There are several different types of radiometers on the market, however, the vacuum photodiode appears to be the one most commonly used.

The instrument itself consists of a probe or sensor and a measuring device or meter to determine how many photons impinge

on the probe. The probe itself incorporates a quartz wide angle diffuser, an interference filter, a blocking filter and a vacuum phototube as the detector. The probe will have a characteristic spectral sensitivity depending on which band of UV radiation one elects to measure. Probes are not interchangeable and measurements of the irradiance of a source must be made with a probe containing the appropriate filter for that source. In our experiments we used a UVX Radiometer (UV Products Inc., San Gabriel, U.S.A.) We used two sensors for calibration namely, a UVX-31 and a UVX-36 sensor. The UVX-31 sensor is designed and calibrated to accurately measure radiation from UVB lamps (310 nm), while the UVX-36 is designed and calibrated to measure 365 nm radiant energy. The absolute spectral response of each is shown in the following two absolute response curves.

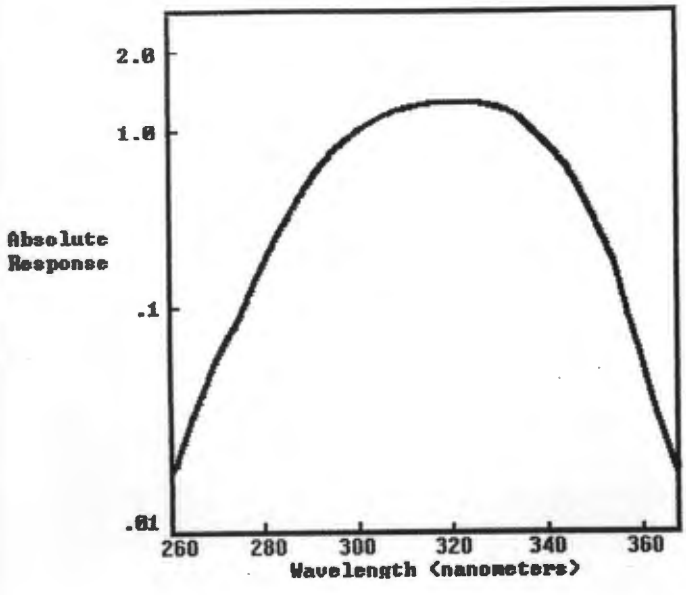

Sensor A. The absolute spectral response of the UVX-31 sensor

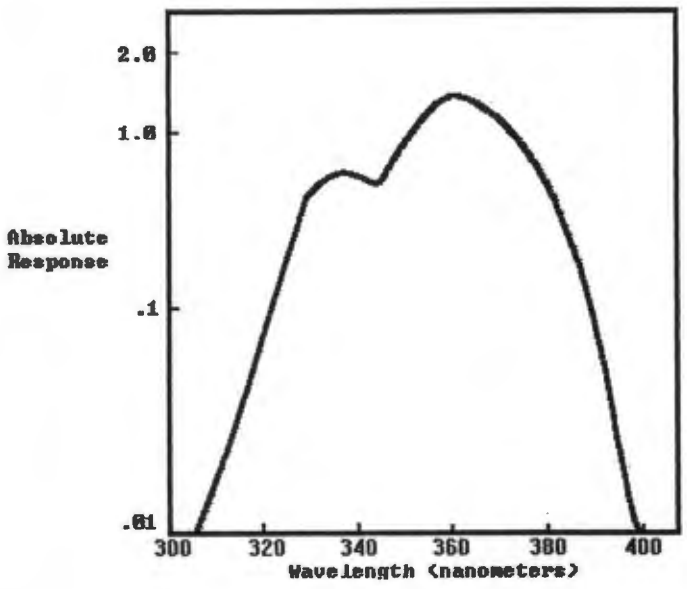

Sensor B. The absolute spectral response of the UVX-36 sensor

4.7.2. Units of measurement

When discussing radiation damage there are several accepted definitions which are widely used, for example:

a) Radiant energy - is the amount of electromagnetic radiation expressed in Joules (J).

b) Radiant power - describes the rate at which the radiant energy is delivered and is expressed in Watts (W) = Joules/sec.

c) Irradiance - is described as the "radiant power" per unit area at a given surface and is expressed in W/cm^2.

d) Exposure dose is the radiant energy delivered per unit area of a given surface in a given exposure time and is expressed in Joules/cm^2 or more commonly as:

Exposure dose = irradiance x exposure time

or:

Exposure dose (Jcm^{-2}) = irradiance (meter reading in uW/cm^2) x exposure time (t in seconds) x 10^{-3}.

4.7.3 Measurements

TABLE IV. Summary of the measured fluorescent lamp output and calculated exposure dose for both the acute and chronic conditions of exposure.

Conditions of exposure	Sensor	Meter reading $\mu W/cm^2$	Exposure duration (t) sec	Exposure dose Jcm^{-2}
3 lamps at 1 meter	UVX 31	28.8	10,800	0.31
	UVX 36	1.1	10,800	0.01
3 lamps at 0.5 meters	UVX 31	76.5	10,800	0.83
	UVX 36	6.6	10,800	0.07
1 lamp at 2 meters	UVX 31	2.3	3,600	0.008
	UVX 36	0	3,600	0
1 lamp at 2 meters	UVX 31	2.3	7,200	0.016
1 lamp at 1 meter	UVX 31	15.5	3,600	0.056
1 lamp at 0.5 meters	UVX 31	48.6	3,600	0.17

Every attempt was made to measure the output of the fluorescent lamps as accurately as possible and in addition the sensor was placed at the position where the rabbit's eye would be during exposure. The calculated exposure dose of 0.31 Jcm^{-2} accumulative over a 3 hour period is well above the rabbit corneal threshold value of 0.0156 Jcm^{-2} determined by Pitts et al (1987) who also stated that the higher the level of exposure, the greater the damage. The exposure dose of 0.31 Jcm^{-2} is sufficiently high to cause the acute damage seen in Figs. 8.4 and 8.5. and is a factor of 20 above threshold.

The peak response of sensor A (UVX-31) at 310-330 nm covers

a significant portion of the UV-B waveband of 290-320 nm. There is a certain amount of overlap into the UV-A and UV-C wavebands however the response of sensor A in these areas is low. The absolute response of sensor B (UVX-36) is maximal at approximately 360 nm which is well into the UV-A radiation band and from Table IV we can see that the calulated exposure dose of 0.01 Jcm^{-2} obtained from the measurements of sensor B confirm that the fluorescent lamps we used in our experiments emit mainly UV-B radiation, and very little UV-A radiation.

RESULTS

5.1. Scanning electron microscopy of the normal rabbit corneal epithelium

When viewed by SEM, the epithelium at low magnification was seen as a flat tightly packed cellular layer with little surface topography (Fig. 8.1 A). The smoothness of the epithelial layer was broken only by the occasional discarded cell, cells that are apparently part of the normal process of epithelial exfoliation. The superficial epithelial layer as seen by SEM showed the cells to be polygonal in nature and characterized as "light", "medium" and "dark", a classification also used by Hoffman (1972), Pfister (1973) and Ringvold (1983). "Dark" cells are thought to represent the hypermature stage of a surface epithelial cell, Hoffman (1972). Similarly Pfister (1973) also suggested that the "dark" cells covering the largest area are the oldest cells and loose their microvilli as they age. In contrast, the smaller "light" cells are those that have just reached the surface and are showing only a small portion of their cell wall. The older "dark" cell gradually peels away and in doing so exposes the new young cell underneath as seen in Fig. 8.2 B.

The epithelial cells were distributed in random fashion over the surface of the cornea, with the "medium" and "dark" cells tending to form clumps and covering the largest area. At higher magnification it becomes evident that all the cells are studded with microvilli and all three types of cells can be seen to possess specific surface features (Fig. 8.1 B; Fig. 8.2 A)

termed "ring-shaped structures" by (Ringvold, 1983). These ring-shaped structures have also been called either full thickness epithelial holes (Pfister, 1973) or superficial impressions (Hoffman, 1972). Under low magnification these ring-shaped structures were found on all three types of cells though they appear more concentrated on the "medium" and "dark" cells. These ring-shaped structures are oval to circular in appearance and range in size from 1 - 5 μm (Fig. 8.3). The rim of these structures is somewhat elevated and appears to be the retracting edge of the plasma membrane (Fig. 8.3). These structures generally are devoid of microvilli though some have been found to contain microvilli (Pfister, 1973).

In this study we did not ever encounter any signs of vasculization or blood cells. Results for this study were taken from the central region of the cornea.

5.1.1. The effects of acute exposure for 3 hours

At low magnification the damage to the cells of the epithelial layer following a 3 hour exposure (0.31 Jcm^{-2}) to UV-B radiation was quite severe (Figs. 8.4; Figs. 8.5). The micrograph in Fig. 8.4 A shows the epithelial layer to be very rough and uneven, most probably a result of cellular oedema. Any inference to "light", "medium" or "dark" cells has become difficult due to the gross distortion of the surface epithelial cells and there are seemingly fewer microvilli left on the cell surface. At higher magnification (Fig. 8.4 B), it can be seen clearly that the swelling of the epithelial cell was severe enough that the

cell membrane ruptured leaving the nucleus lying exposed on the surface (Fig. 8.4 B). This "bulging" out of the cell nucleus, probably due to oedema, was also reported by Ringvold (1983) who referred to these severely distorted cells as "spheroid bodies". There is also evidence of some deep holes in the epithelial layer extending down into the underlying polyhedral layer (Fig. 8.4 B). This degree of destruction has not been reported before by either Ringvold (1983) or Hoffman (1972), in corneas from rabbits similarly subjected to ultraviolet radiation. A definite increase in the number of partially and completely discarded cells was also evident (Fig. 8.5 B). Occasionally we found areas where the swelling had caused the normally tight cell to cell boundary to separate (Fig. 8.5 A).

Although the swelling is severe, many cells retain their microvilli (Fig. 8.5 A). The number of ring-shaped structures seen in abundance in the normal epithelial layer have been greatly reduced, another morphological indication of radiation damage. The absence of these ring-shaped structures was also observed by Ringvold (1983) after only 30 minutes of exposure to UV radiation. This then supports our own observation after 3 hours of radiation trauma.

5.1.2 The effects of acute exposure for 3 hours plus 3 hours recovery

The 3 hour recovery period, following acute exposure, resulted in certain regenerative signs such as: less swelling overall, more defined cells and cell borders and many more cells

being discarded which is an indication of rapid cell regeneration. In fact, it appears that a good portion of the superficial cells were at some stage of either being partially discarded or completely discarded. This was also reported by Ringvold (1983), who observed a similar result 3 hours after UV-irradiation. Although there were signs of a definite decrease in the gross swelling of the epithelial cells, cellular oedema was still apparent. Several signs of the trauma caused by ultraviolet radiation persist and become evident at higher magnifications. Typically these features include fine cracks and even holes covering the surface of several of the superficial cells (Fig. 8.6 B). These so called "plasma membrane defects" were also reported by Ringvold (1983) and they are seen primarily in the desquamating cells. The "plasma membrane defects" may also be present in cells covered with microvilli, since the microvilli may be obscuring them.

5.1.3 The effects of acute exposure for 3 hours plus 16hours recovery

After the longer recovery period of 16 hours the epithelial layer is showing further signs of smoothing out and the bulging in the nuclear region is less pronounced. However, there were still many cells at different stages of desquamation most probably because the cells damaged in the deeper layers of the epithelium are making their way to the surface and then being discarded.

A further sign of regeneration by the epithelial cells is the apparent absence of the plasma membrane defects seen so clearly in the previous micrograph (Fig. 8.6 B). However, the cells still do not show the tight integrity one associates with the normal epithelial layer (Fig. 8.1) although cell to cell contact appears to be improving. The cells may be identified, as before as "light", "medium" and "dark", although the cells seen in Fig. 8.7 are mainly of the "light" to "medium" variety. These cells are heavily covered with microvilli. The "dark" cells are not as apparent at this stage. We would expect an abundance of older "dark" cells since the epithelial layer is still in a state of rapid repair and there are plenty of cells at some stage of being discarded. It is possible that there is an over abundance of new "light" cells due to the rapid turnover of the surface epithelial cells. It is also possible that there is a lack of definition between the cells due to the inherently low contrast of the specimen which is not uncommon when dealing with a very flat sample. Due to the nature of the specimens, we had no way of producing samples with more topography. Even after recovering for 16 hours the ring-shaped structures had not reappeared indicating that the epithelial layer may still be a long way from recovering to its normal state.

5.1.4. The effects of acute exposure for 3 hours plus 21 hours recovery

At low magnification the epithelial layer after recovering for 21 hours is covered extensively with "dark" cells (Fig. 8.8), most of which have few if any microvilli . A slight bulge in the

nuclear area is still apparent and appears more prominent in the "dark" cells.

The ring-shaped structures have also reappeared but are not as numerous and wide spread as in the normal epithelial layer. Cell to cell contact seems much better and prominent cell outlines are again visible. There is no evidence of any plasma membrane defects or any other surface holes.

6.1. The effects of chronic exposure for 119 days

The scanning electron micrographs of the chronically exposed cornea (Fig. 9.1 and Fig. 9.2) show that a cumulative daily radiation dose (1 tube x 1 hour at 2 meters distance for 107 days plus 1 tube x 2 hours at 2 meters distance for 12 days) has had a limited effect on the corneal surface epithelial layer. The exposure periods of 107 and 12 days were choosen arbritarily. We decided that since there were no clinical signs of damage after 107 days that the dose should be increased over a shorter period of time. Time constraints necessitated the completion of this study.

The surface epithelial layer did not appear quite as flat and smooth as the control cornea however, the differences were marginal. There appears to be a predominance of "dark" cells which could be a result of radiation damage but this criteria by itself is by no means conclusive. If one looks at the control epithelial layer (Fig. 8.1 A), one can also see many areas where

there is a predominance of "dark" cells. A difference one can see is that the nuclei of many of the "dark" cells are very slightly raised, a morphological condition not observed in the control "dark" cells.

At the higher magnification the cells appear almost identical to normal control cells, with well defined cell borders and an abundance of surface microvilli. The characteristic ring-shaped structures are still plentiful though actual numbers per unit area seem to be slightly less than in the control cornea, though this may be a somewhat objective observation. Otherwise the cells appear very close to the normal epithelial layer and could easily be identified as such.

6.1.1. The effects of chronic exposure for 144 days

In this experiment the rabbit was exposed daily for the longer period of 144 days at an exposure dose of 0.016 Jcm^{-2} (TABLE IV), or (1 tube x 2 hours at 2 meters distance). At low magnification the epithelial layer (Fig. 9.2A) appeared more uneven than in the previous (Fig. 9.1A), with many cells starting to peel away or in the process of being discarded. Another morphological indication of cellular damage and subsequent oedema were the cracks that had formed at some of the cell boundaries. At the higher magnification there were no ring-shaped structures visible and the nuclei of some cells were bulging noticeably. The distinction between "light", "medium" and "dark" cells is also not readily apparent.

Figure 8.1 **Scanning electron micrographs of the epithelial layer of a normal rabbit cornea illustrating the different cell types and their distribution at different magnifications**

A) At low magnification the cells of the epithelium are characterized as "light (L), "medium" (M) and "dark" (D).
Scale represents 50 μm. Mag 404x

B) Higher magnification of the epithelial layer to show the distribution of the ring-shaped structures (Ri) common to the surface epithelial cells. The cells appear flat, tightly knit with well defined cell borders (B).
Scale represents 100 μm. Mag 805x

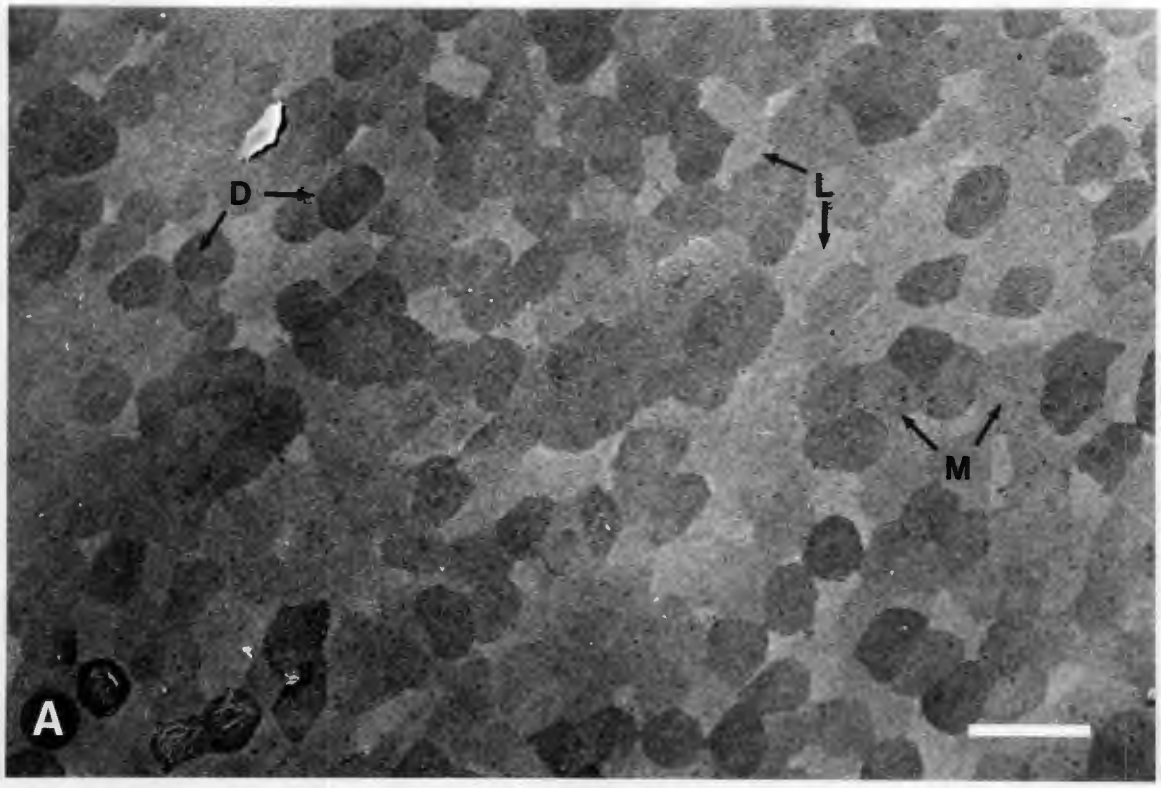
D
L
M
A

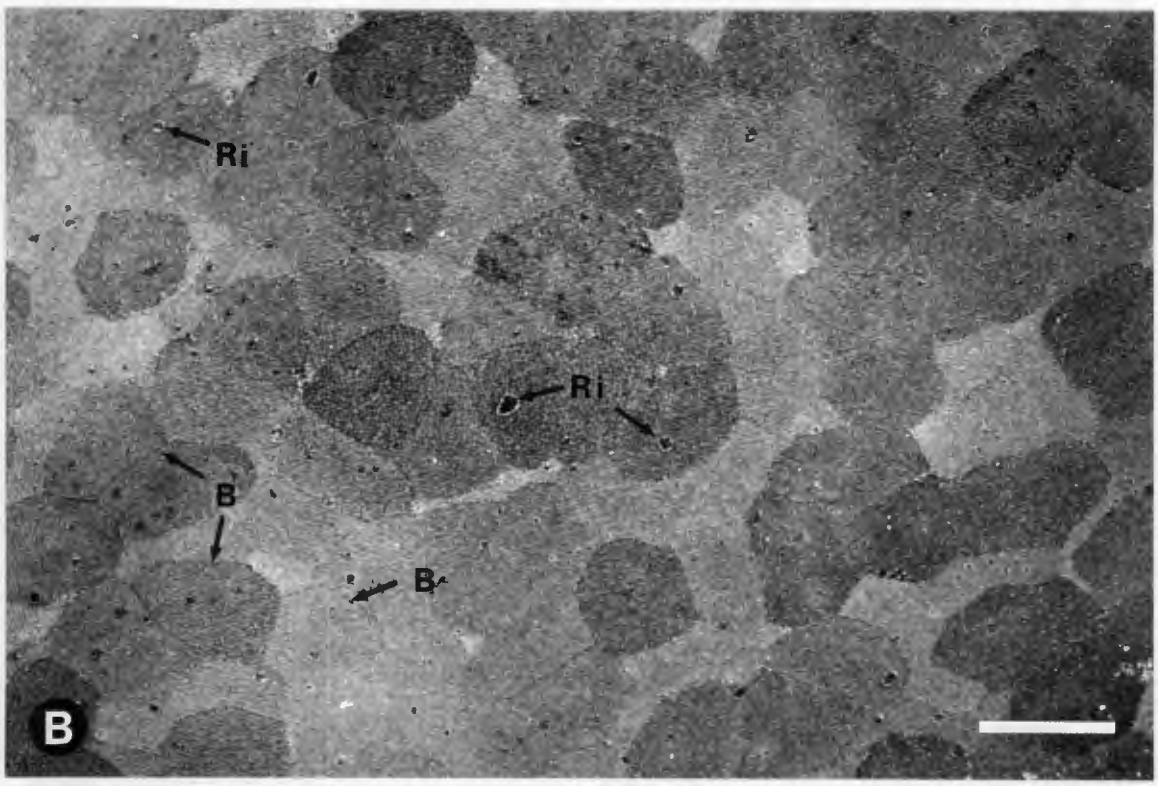
Ri
Ri
B
B
B

Figure 8.2 **Scanning electron micrographs of the epithelial layer of a normal rabbit cornea illustrating the process of cell desquamation**

A) Cornea epithelial cells at apparently different stages of development. A "dark" cell (D) with several ring-shaped structures (Ri) on its surface is thought to represent a hypermature stage of a surface epithelial cell. A "light" (L) cell has replaced the surface cell being discarded (C). Another "light" (L) cell is located immediately adjacent the "dark" (D) cell. Cell borders (B) are clearly defined.
Scale represents 10 μm. Mag 3200x

B) An example of an epithelial cell in the process of being discarded (D). The cell is gradually peeling away and exposing the "light" (L) cell underneath.
Scale represents 5 μm. Mag 6600x

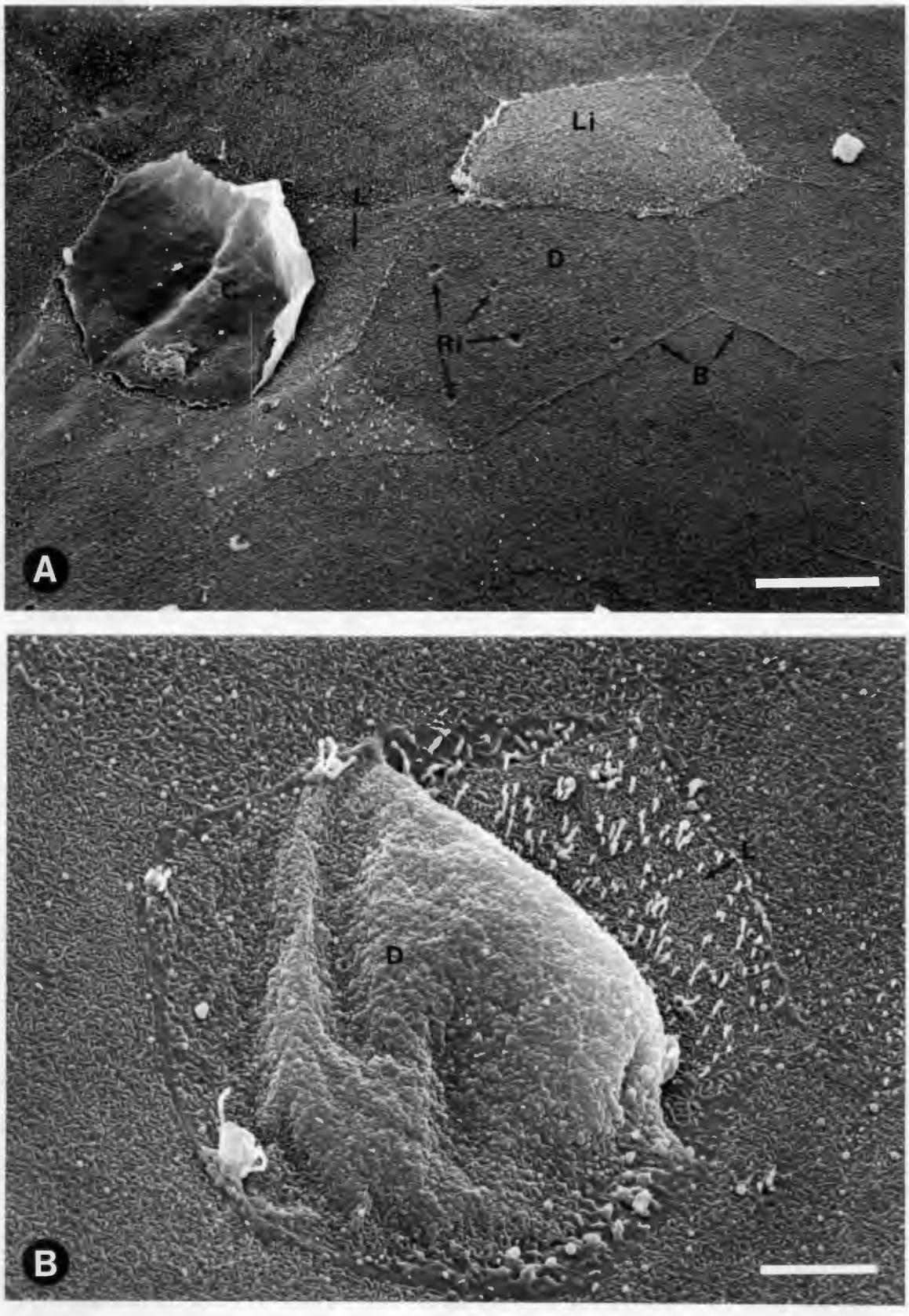
Li
L
D
Ri
B
A
L
D
B

Figure 8.3 **High magnification scanning electron micrograph of the epithelial layer of a normal rabbit cornea showing the distribution of surface microvilli**

High magnification of "light" (L), "medium" (M) and "dark" (D) cells to show visually the difference between the three types of cells. The "light" (L) cell has a surface that is densely packed with microvilli and appears to have more microvilli per unit area than either the "medium" or "dark" cell. The "medium" and "dark" cells only appear to have fewer microvilli probably due to a thicker surface mucin layer. Several ring-shaped structures (Ri) can also be seen. The bright spherical structures (Sp) dispersed across the surface are most probably globules of mucin.
Scale represents 2 μm. Mag 17180x

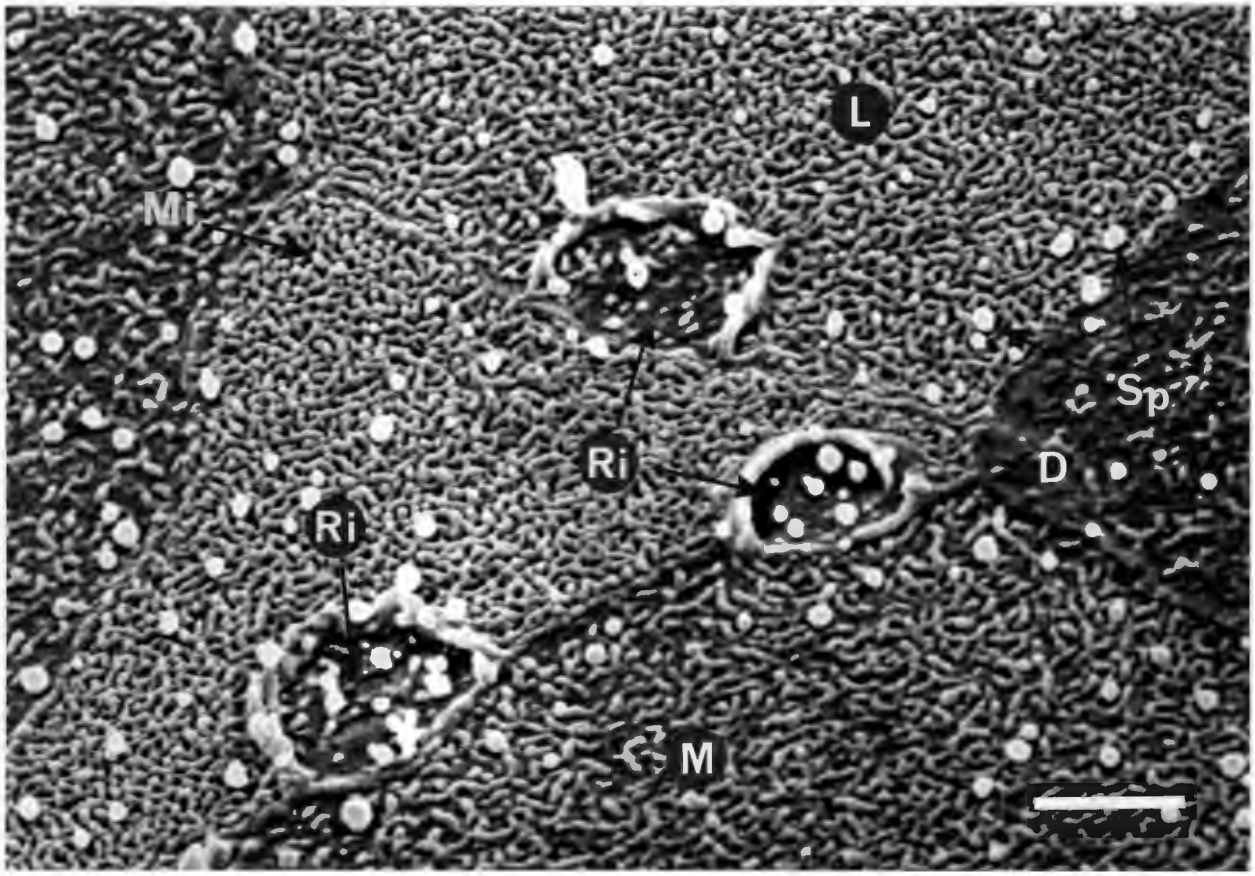
L
Mi
Sp
Ri
D
Ri
M

Figure 8.4 **Scanning electron micrographs of the rabbit corneal epithelial layer after 3 hours exposure to UV-B radiation showing gross cellular damage at different magnifications**

A) Low magnification micrograph of the epithelial layer immediately after 3 hours exposure. "Light", "medium" and "dark" cell distinction is no longer apparent. Surface cells (C) appear rounded and elevated above the surface. Irregular surface holes (Ho) had appeared on the surface. Cell outlines are also no longer apparent.
Scale represents 100 μm. Mag 490x

B) High magnification of the surface to show the surface holes (Ho) seen above.
Scale represents 10 μm. Mag 3250x

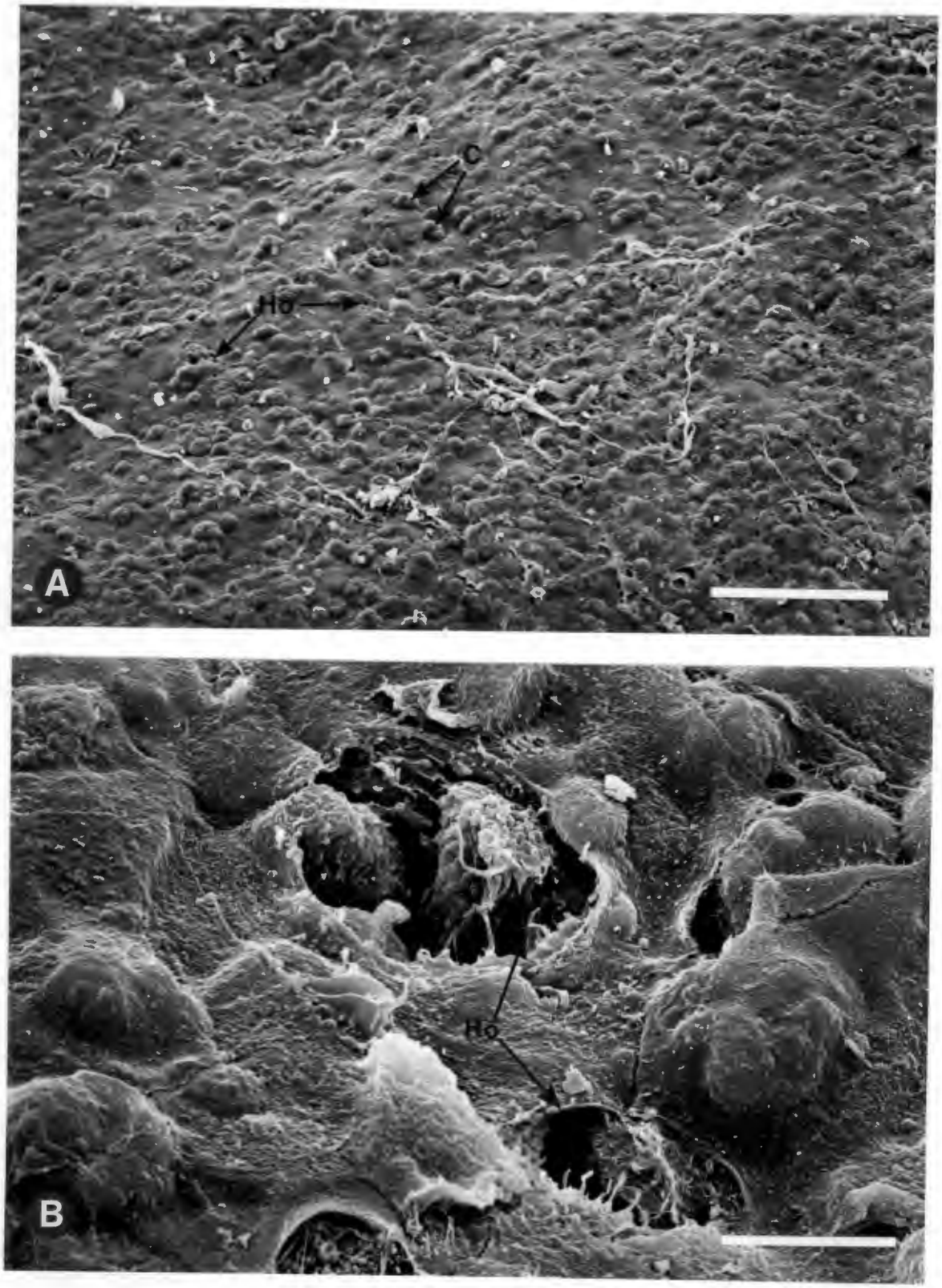
C
Ho
A
Ho
B

Figure 8.5 **Scanning electron micrographs of the rabbit corneal epithelial layer after 3 hours exposure to UV-B radiation to show the extent of cellular damage at high magnification**

A) High magnification to show more signs of damage after 3 hours exposure. Two completely discarded (D) and two partially discarded (Di) cells in close proximity. In some cases the cells had separated (S) from one another, most probably a result of cellular oedema.
Scale represents 10 μm. Mag 3476x

B) Another example of extensive damage where the cells have ruptured exposing the nuclei (Nu) to the surface. Several holes (Ho), quite different from the ring-shaped structures seen in the control cornea are also present.
Scale represents 10 μm. Mag 3150x


D
S
Di
A

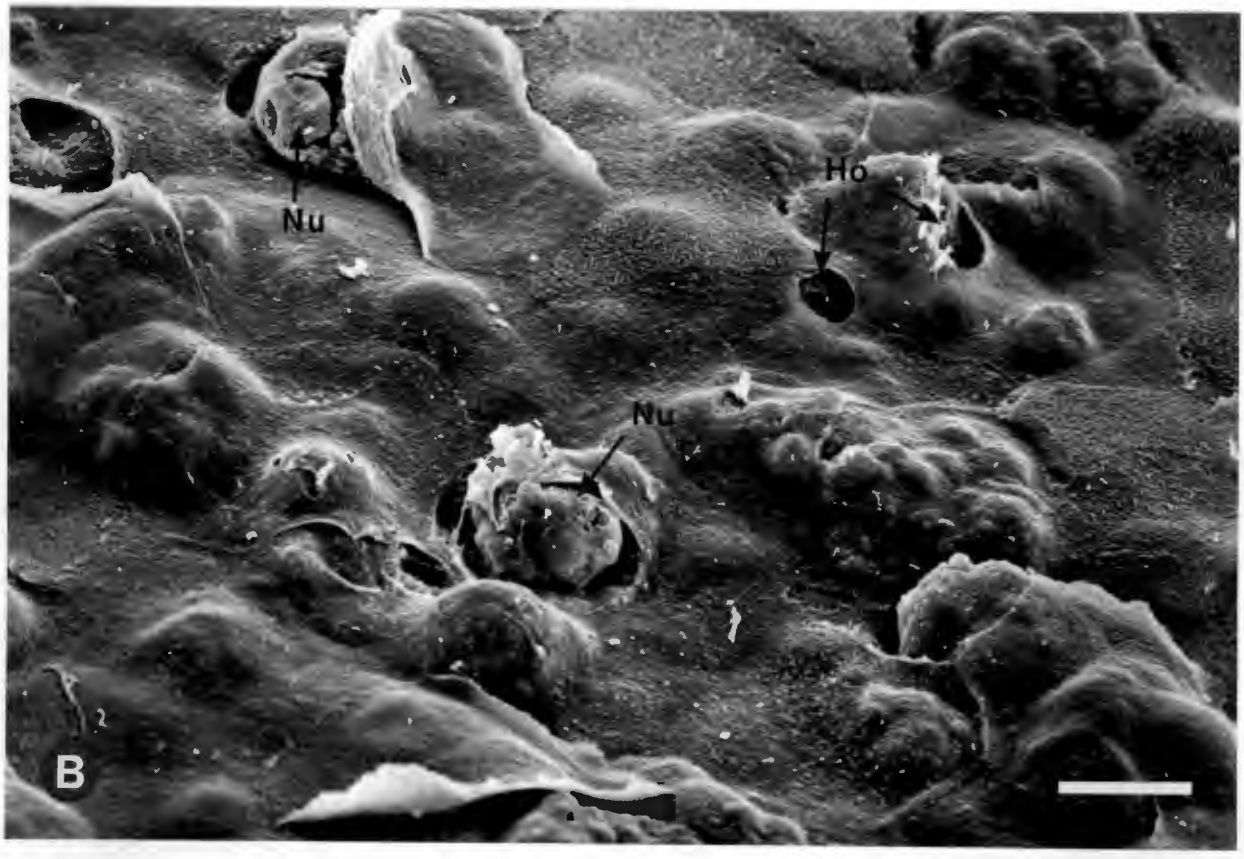
Nu
Ho
Nu
B

Figure 8.6 **Scanning electron micrographs of the rabbit corneal epithelial layer after 3 hours exposure to UV-B radiation, followed by 3 hours recovery to show the effects of the radiation damage at different magnifications**

A) At low magnification the surface epithelial layer is showing signs of increased exfoliation with many discarded (D) and partially discarded (Di) cells over much of its surface. Cell borders (B) appear clearer and more defined, though the uneven appearance of the surface suggests that some oedema is still in effect.
Scale represents 50 μm. Mag 600x

B) High magnification of surface epithelial cells showing marked plasma membrane defects (De) which appear as fine cracks over the entire surface of the cell.
Scale represents 10 μm. Mag 2300x

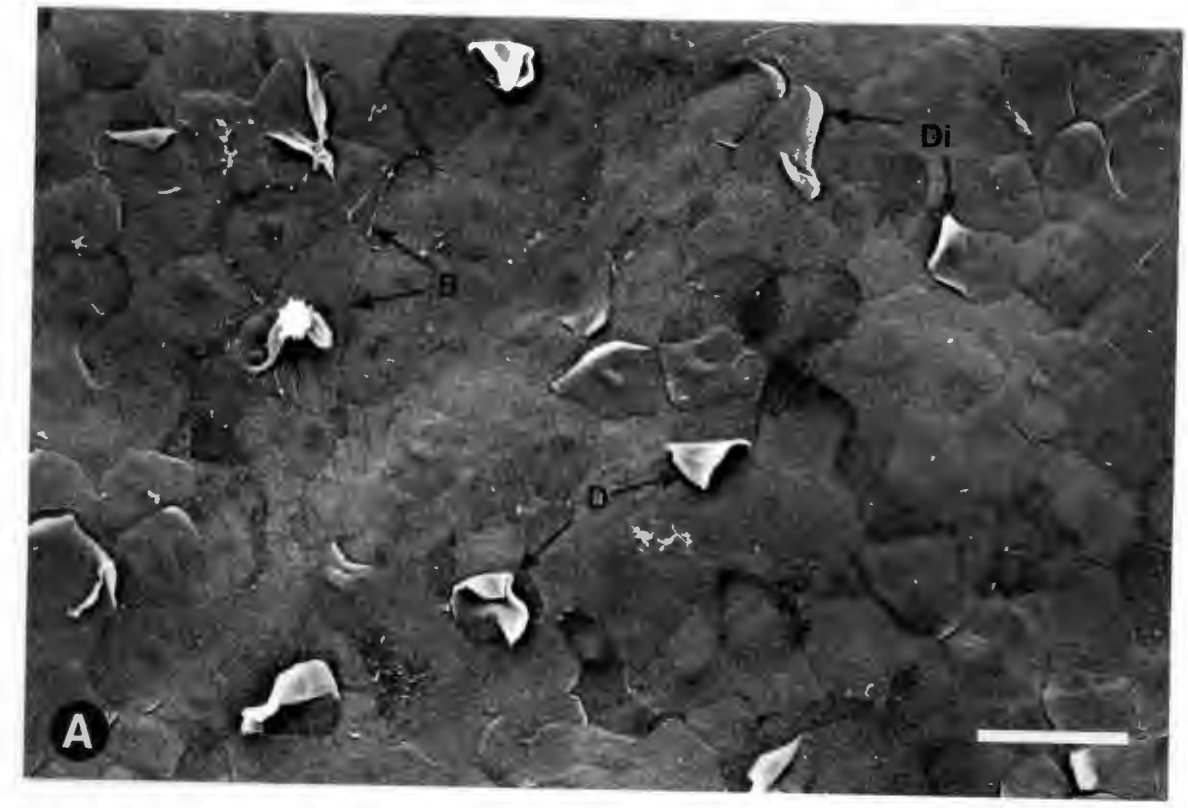
Di
B
D
A


De
De
B

Figure 8.7 **Scanning electron micrographs of the rabbit corneal epithelial layer after 3 hours exposure to UV-B radiation, followed by 16 hours recovery illustrating the reappearance of characteristic cells**

A) The surface epithelial layer appears smoother, though partially discarded (Di) cells were still in abundance. "Light" (L), "medium" (M) and "dark" (D) cells can again be identified.
Scale represents 50 μm. Mag 593x

B) High magnification of the boxed area in A. The "light" young cells are covered with microvilli. Ring-shaped structures have not yet appeared, though the cells appear tightly packed with well defined cell borders (B).
Scale represents 25 μm. Mag 2060x

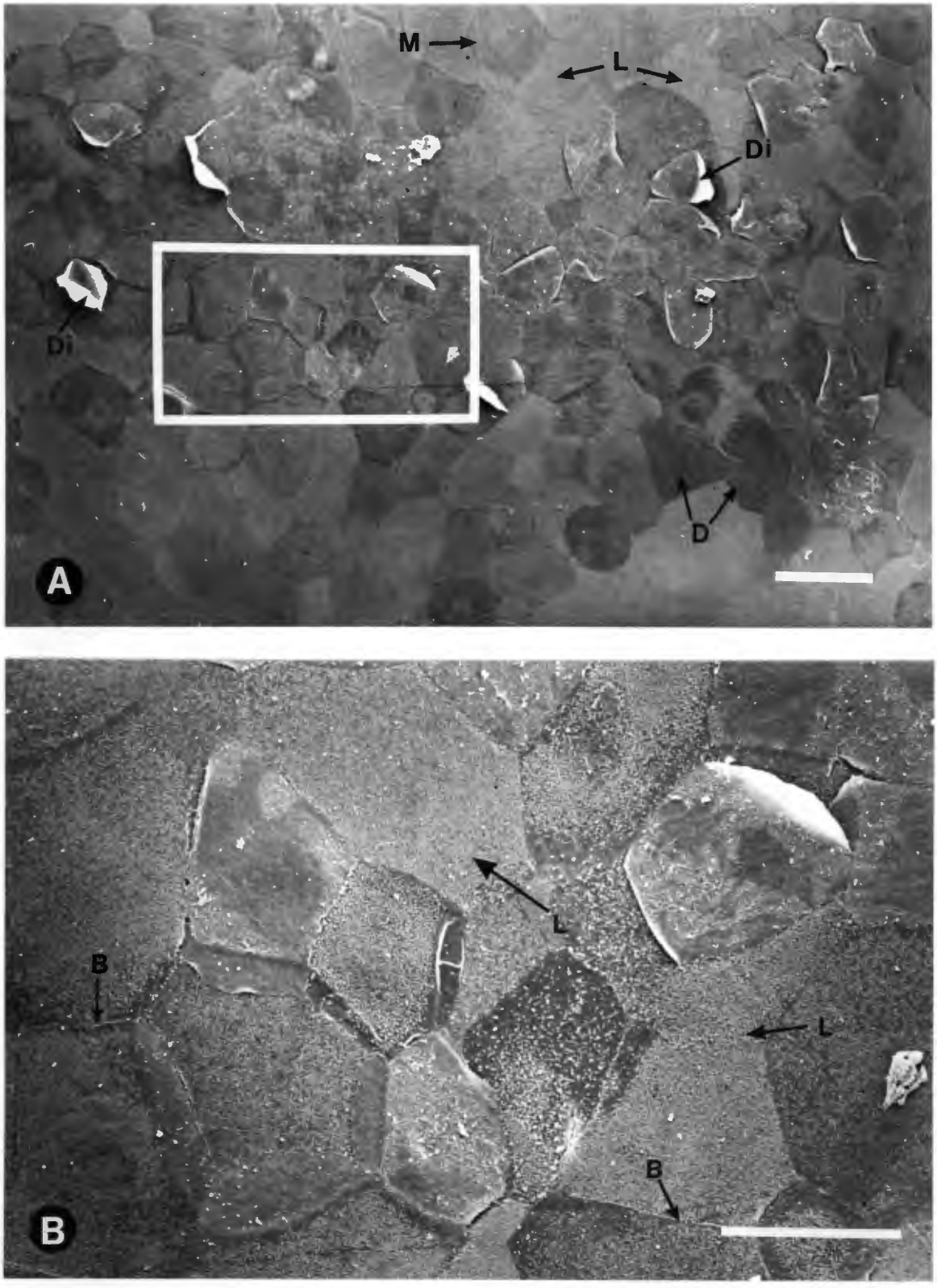
M
L
Di
Di
D
A
L
B
L
B
B

Figure 8.8 **Scanning electron micrographs of the rabbit corneal epithelial layer after 3 hours exposure to UV-B radiation, followed by 21 hours recovery showing the return of features seen in the control**

A) Low magnification micrograph of the epithelial layer showing a predominance of "dark" (D) cells after 21 hours recovery. Partially discarded (Di) cells are still abundant.
Scale represents 100 μm. Mag 560x

B) At a higher magnification one can again see ring-shaped structures (Ri). The nuclei (Nu) of the "dark" cells are slightly elevated, an indication that the swelling had not yet totally subsided.
Scale represents 25 μm. Mag 2170x

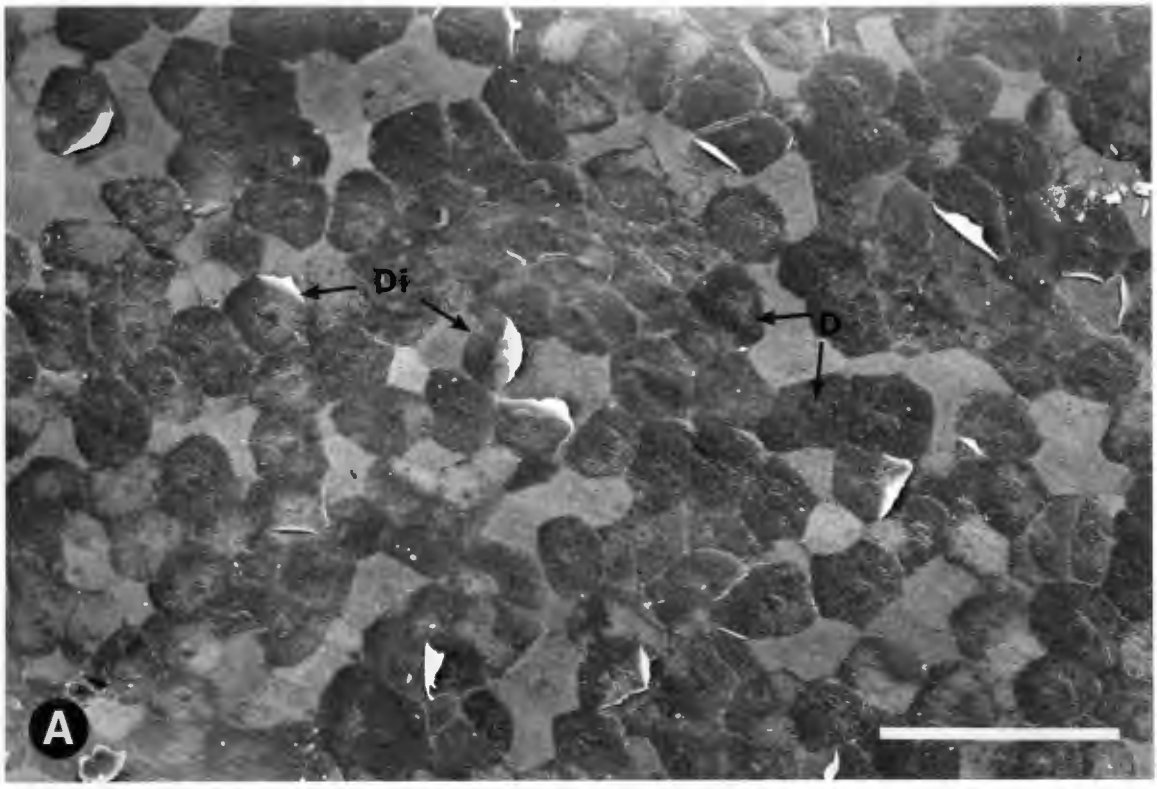
Di
D
A

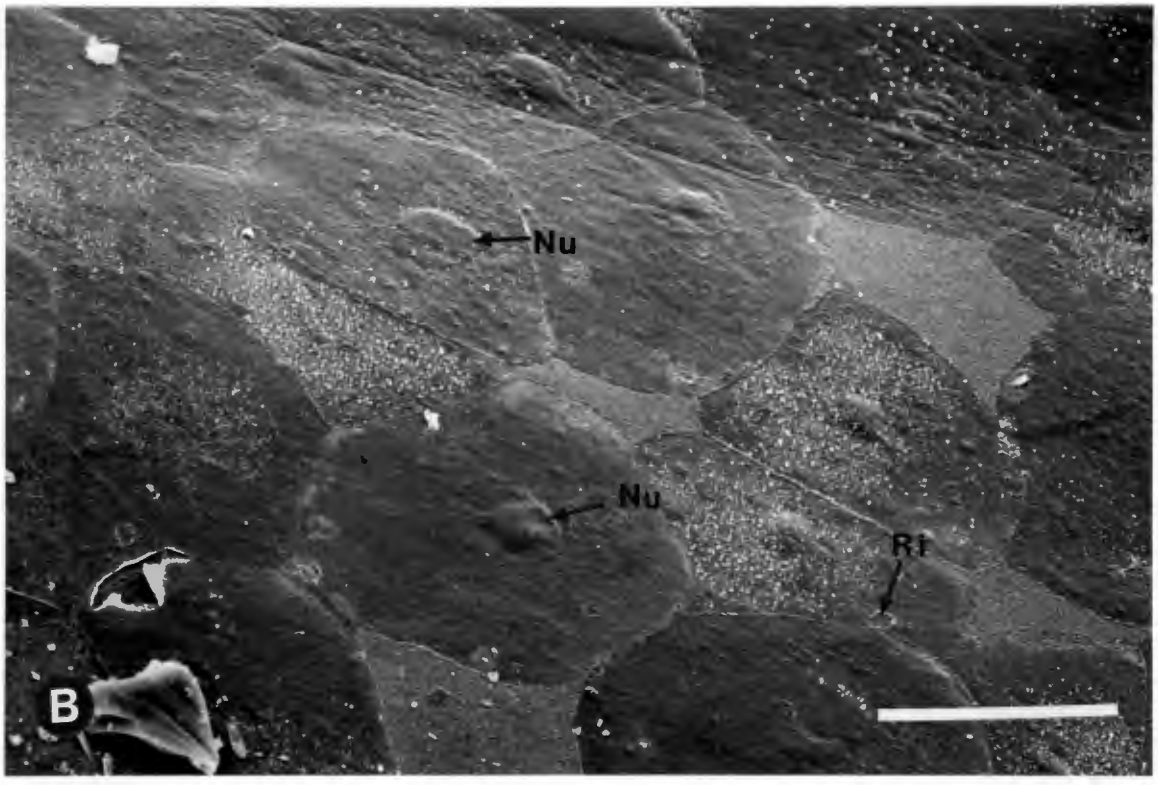
Nu
Nu
RI
B

Figure 9.1 **Scanning electron micrographs of the rabbit corneal epithelial layer after daily chronic exposure for 119 days to illustrate some apparent damage due to accumulative radiation effects**

A) Low magnification micrograph of the corneal epithelial after daily exposure for 119 days showed the surface to be covered with predominantly "dark" (D) cells. The surface appears very flat and smooth though some slight bulging in the nuclear (Nu) region was apparent.
Scale represents 100 μm. Mag 690x

B) At higher magnification several "dark" (D) cells are seen surrounded by "light" (L) cells. Both "light" and "dark" cells had ring-shaped structures (Ri) on their surface.
Scale represents 25 μm. Mag 2700x

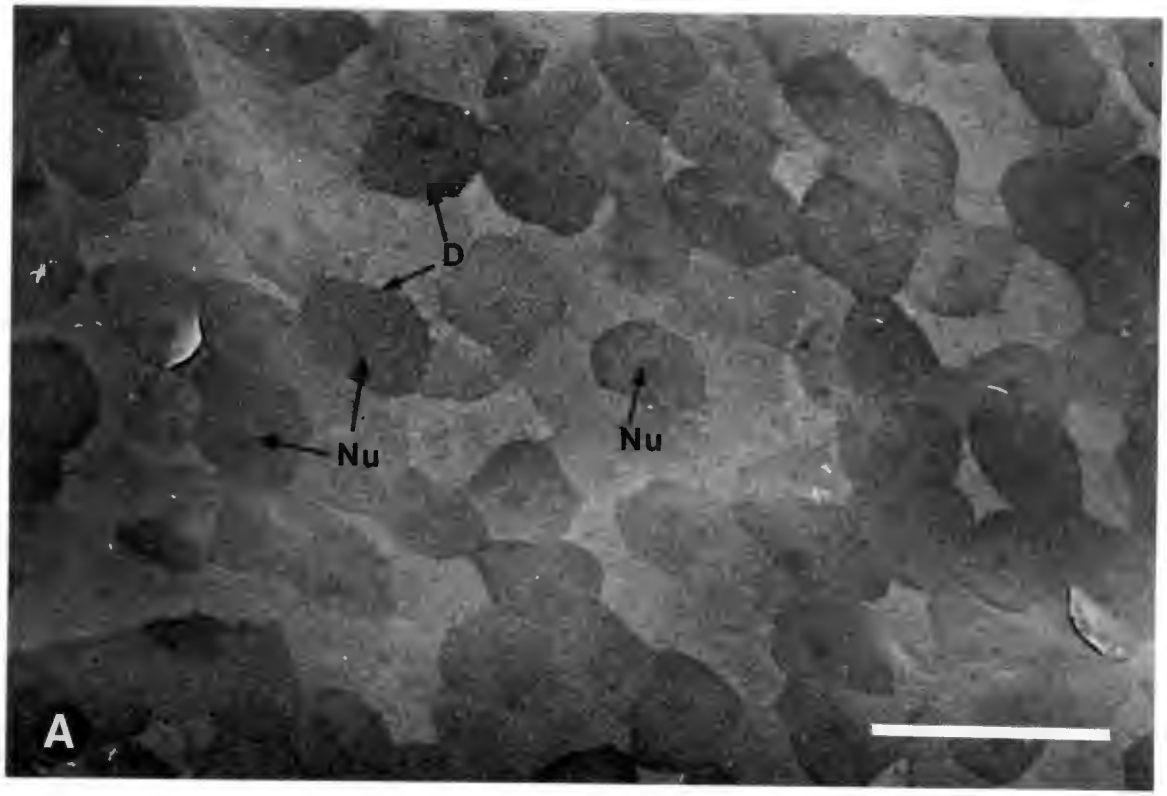
D
Nu
Nu
A

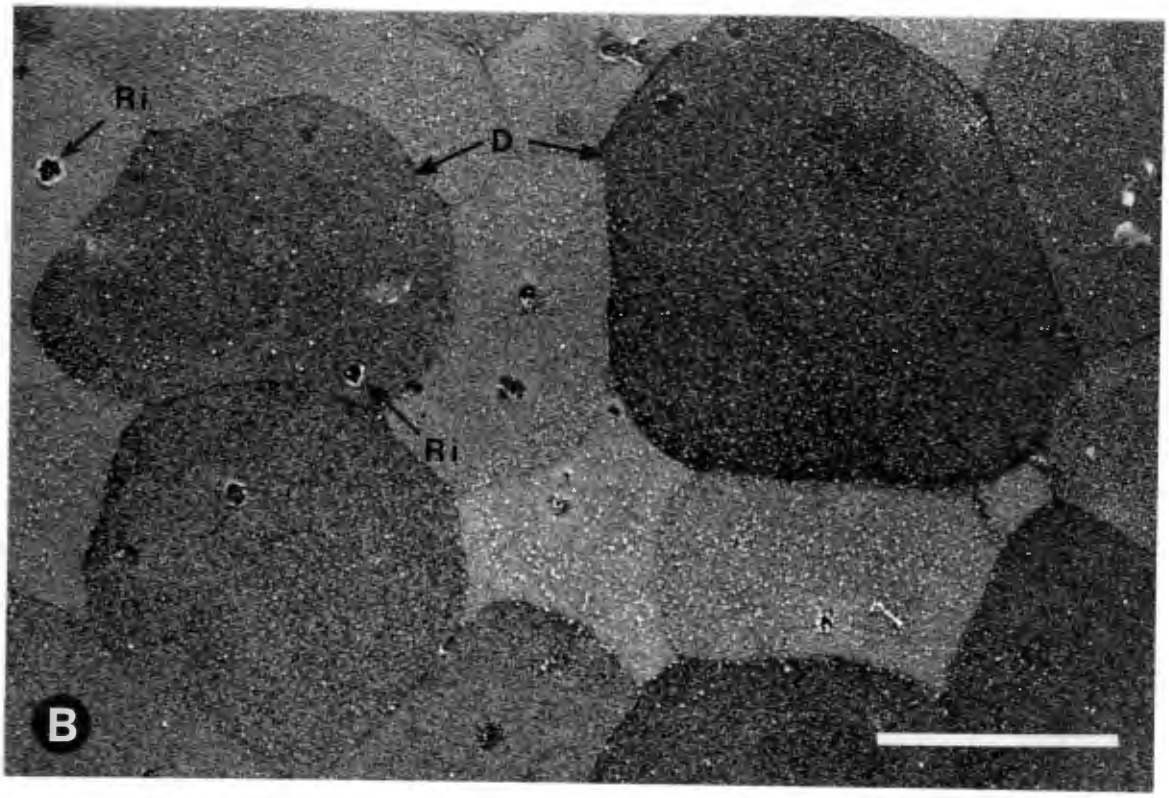
Ri
D
Ri
B

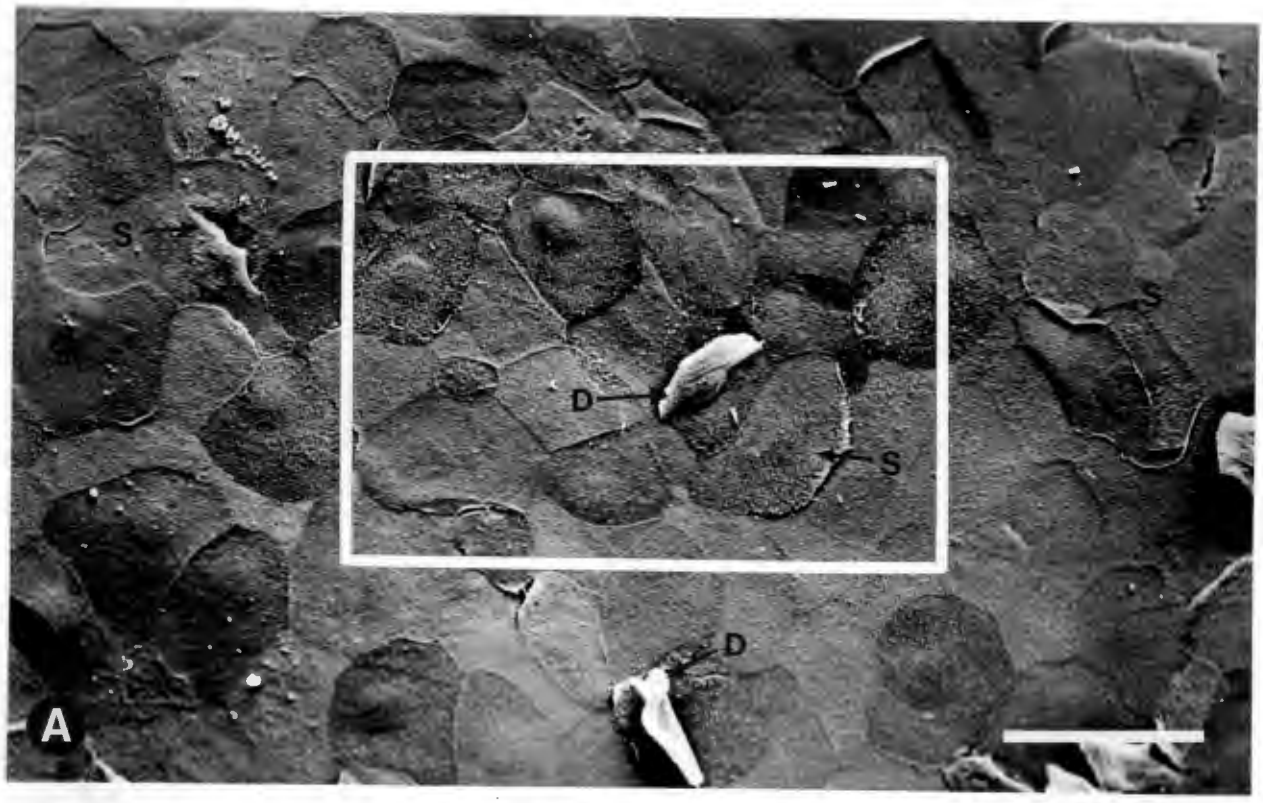
S
D
S
S
D
A


Nu
S
C
C
S
C
B

7.1. Transmission electron microscopy of the normal rabbit corneal epithelium

To determine whether the UV radiation also caused damage to the deeper cell layers of the epithelium (not seen in the SEM) and to verify some of our results, we also performed transmission electron microscopy on the same corneal tissue samples. Prior to cutting thin sections for transmission electron microscopy, a semi thin section was cut (Fig. 10.1) to check the orientation and quality of the processed material.

A representative cross section through the normal epithelium seen in Fig. 10.2, shows the three distinct cell layers which make up the epithelium. The outer layer is made up of several layers of thin and elongated squamous epithelial cells, with poorly outlined nuclei that have their long axis parallel to the surface of the cornea. The inner polyhedral layer located immediately beneath the squamous layers is itself made up of only one to two cell layers. The cells in this layer contain nuclei that are for the most part spherical and often have irregularities in their profiles. The cytoplasm appears dense with few organelles visible even at low magnification. Finally, the innermost basal layer is composed of a single row of columnar shaped epithelial cells which have elliptical to spherical nuclei orientated with the axis of the cell and perpendicular to the corneal surface. The cells of all three layers are very closely knit with little intercellular spaces, a structural characteristic also seen in the SEM micrographs of

the normal rabbit cornea (Fig. 8.1). The cell membranes of adjacent cells in all three layers form projections that interdigitate with each other which gives the cells the appearance of being highly convoluted.

7.1.1 The effects of acute exposure for 3 hours

The epithelium is showing some signs of damage, though the severe morphological damage observed in the scanning electron micrographs of Figs. 8.4 and 8.5 is not readily apparent in the transmission micrographs. The epithelial layer overall appears to be thinner and the innermost basal cells are no longer columnar shaped and have nuclei orientated parallel to the surface of the cornea. Some of the cells in the inner polyhedral layer appear abnormal, showing signs of apparent cytoplasmic degeneration (Fig. 10.3 A). One such cell (Fig. 10.3 B) shows both cytoplasmic and nuclear degeneration. In addition, the epithelium can no longer be clearly divided into three distinct and separate cell layers, though many of the individual cells still appear normal. Some of the cells also show an unusually high accumulation of peculiar membraneous vesicles in the cytoplasm (Fig. 10.3 A). The appearance of a dead cell almost devoid of cytoplasm directly beneath a superficial dead cell suggests that radiation damage was not limited to the outer surface cell layer.

7.1.2. The effects of recovery periods after acute exposure

In the first experiment where the cornea was allowed to recover for three hours, then removed and processed for transmission electron microscopy, some discrete ultraviolet damage was apparent. For example, several cells in the inner layer were separated by unusually large space formations (Fig. 10.4), which may be histological manifestations of cellular oedema. Similar formations were not observed in the control cornea (Fig. 10.2). It may be argued that these space formations are the same as the vacuole like structures seen in Fig. 10.6 B, though subtle differences such as size, location and material content may suggest otherwise. In addition the varying electron densities of the cytoplasm of some cells may be another discrete sign that ultraviolet radiation has damaged the cells in the inner polyhedral and lower basal layer. However the nuclei of these same cells appear intact and essentially normal.

In two further experiments the cornea was allowed to recover for 16 and 21 hours respectively after which thin sections were examined for any signs of ultrastructural damage. No visible damage was apparent after recovery for 16 hours, though there is still an accumulation of what appear to be membraneous vesicles in the innermost epithelial cells (Fig. 10.5 A). The squamous cell layers appear normal and a single cell about to be discarded is seen on the surface. Most of the morphological damage observed in the 3 hour acute sections (Fig. 10.3) seems to have been repaired though the epithelium is not yet clearly divided into its three distinct layers.

In the section following 21 hours of recovery (Fig. 10.5 B) the epithelium is appears essentially normal, with closely knit cells throughout and dense cytoplasm in all the cells. The nuclei appear normal and even the basal cell nuclei are orientated perpendicular to the corneal surfaceas as in the control cornea

7.1.3. The effects of chronic exposure for 119 and 144 days

The epithelium did not appear damaged to any great extent after 119 days of accumulative radiation (TABLE IV p.52) and for the most part the cell layers were well defined (Fig. 10.6 A). This is not unexpected as the SEM results also showed little direct evidence of any sustained morphological damage. There were however, numerous membrane fragments scattered throughout some cells in all three layers. It is possible that these fragments may be part of the normal composition of the cell. Aside from these fragments the entire epithelium appears normal throughout.

In the second chronic experiment the epithelial cells after being subjected to an accumulative radiation dose (TABLE IV p. 52) over 144 days did show some apparent ultrastructural damage (Fig. 10.6 B). For example, the cells were found to contain vacuole like structures throughout the cytoplasm, some of which appear empty, while others were partially filled with some electron dense material of unknown origin. It may be argued that these vacuole like structures are the same as the space formations in Fig. 10.4, though subtle differences such as size, location and material content would suggest otherwise. The nuclei of these same cells are normal in appearance though the surrounding cytoplasm had a patchy inconsistent texture. It is not possible at this time to determine whether these vacuole like

structures are true manifestations brought about by the accumulative effect of the ultraviolet radiation or whether they are simply artifacts incurred during processing.

Figure 10.1 The corneal epithelium of a normal rabbit cornea as seen by oil-immersion light microscopy in a 1μ thick Epon/Araldite section. The section was cut and then stained with toluidine blue to determine the quality of the embedding. The three cell layers of the epithelium are clearly visible, Squamous epithelial layer (Sq), Polyhedral epithelial layer (Po) and the Basal epithelial layer (Ba).

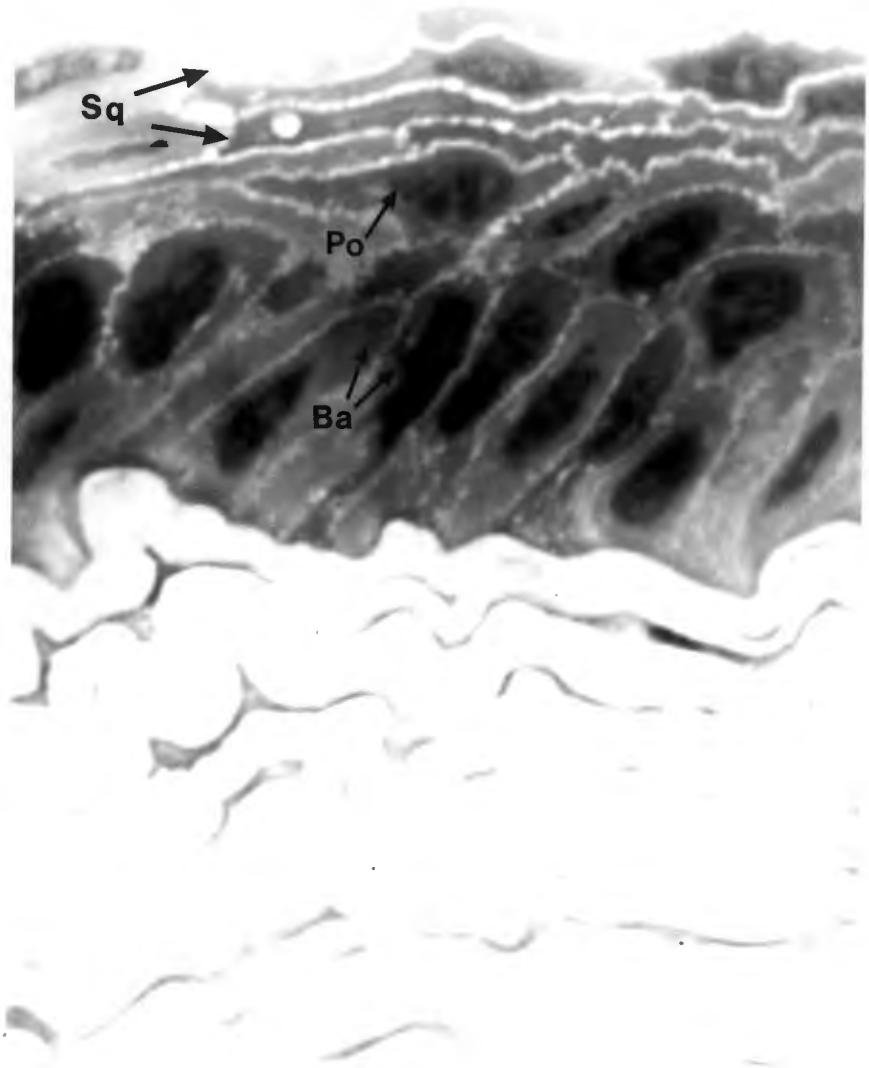
Sq
Po
Ba

Figure 10.2 **Transmission electron micrograph of the normal rabbit corneal epithelial layer at low magnification to show the three epithelial cell layers**

Low magnification micrograph of the epithelium in cross section to show the three distinct cell layers: the outer squamous (Sq) cell layer, the inner polyhedral (Po) cell layer, and the lower columnar-shaped basal (Ba) cell layer.
Scale represents 2 μm. Mag 7740x

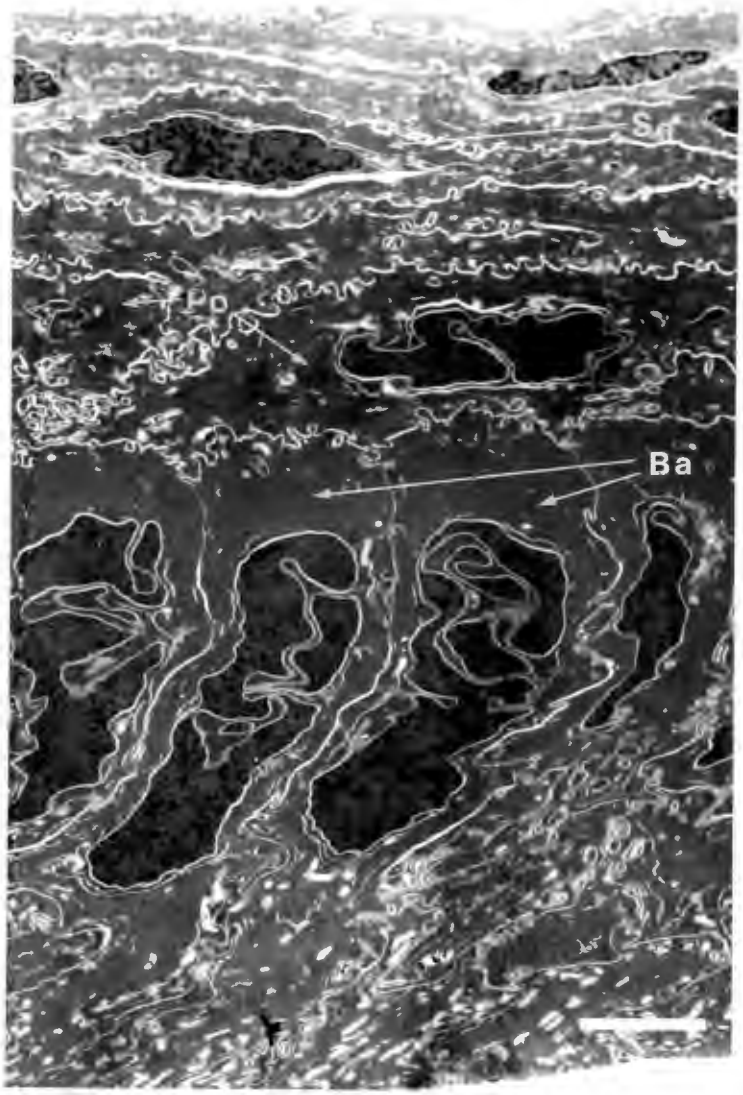
Sf
Ba

Figure 10.3 **Transmission electron micrographs of the rabbit corneal epithelial layer show a thinning of the epithelium and ultrastructural damage after 3 hours exposure to UV-B radiation**

A) Low magnification of the epithelium in cross section. The nuclei of the basal cells (Ba) are now orientated parallel to the corneal surface, not perpendicular. The three cell layers are no longer clearly defined and appear thinner. The cytoplasm (C) of some cells in what should be the polyhedral layer appears thin and granular. A squamous (Sq) epithelial cell is seems ready to be discarded prior to it reaching the surface. Numerous membraneous (Me) vesicles have appeared in the cytoplasm of several cells.
Scale represents 2 μm. Mag 8200x

B) Higher magnification of an abnormal cell in the inner cell layer. The cytoplasm (C) and the nuclear (Nu) material seem to have degenerated. An adjacent cell contains numerous membraneous (Me) vesicles.
Scale represents 1 μm. Mag 12400x

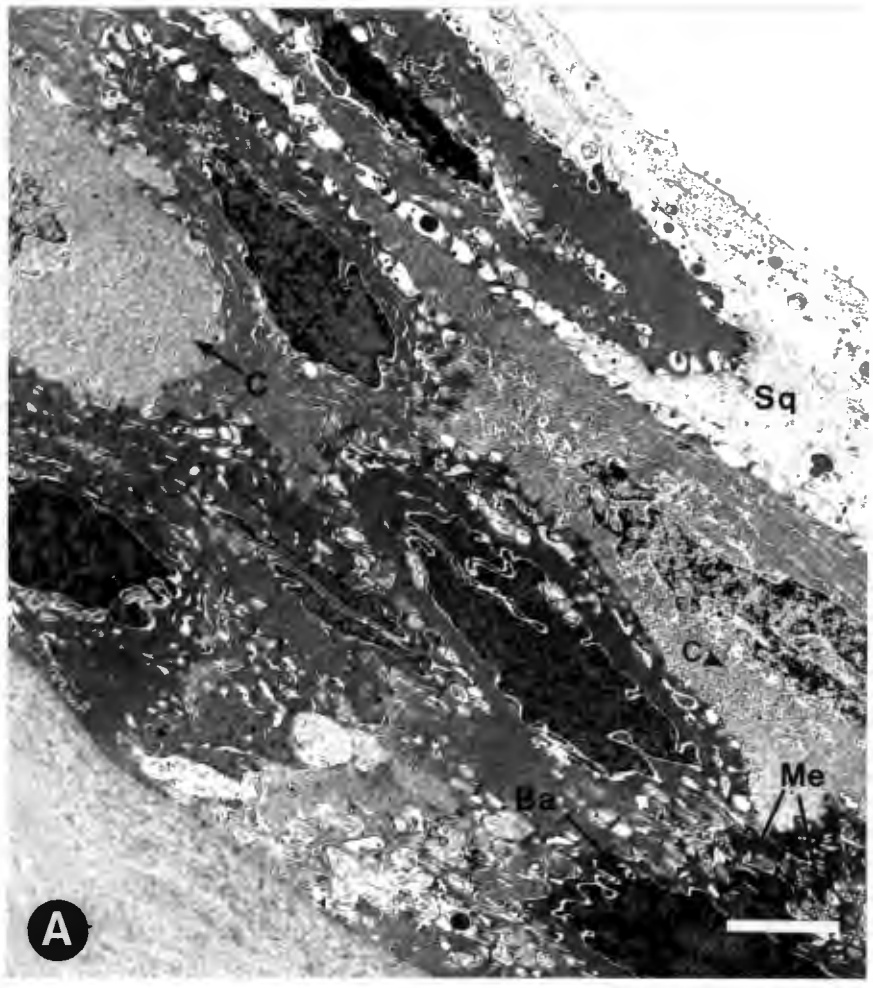
C
Sq
C
Me
Ba
A

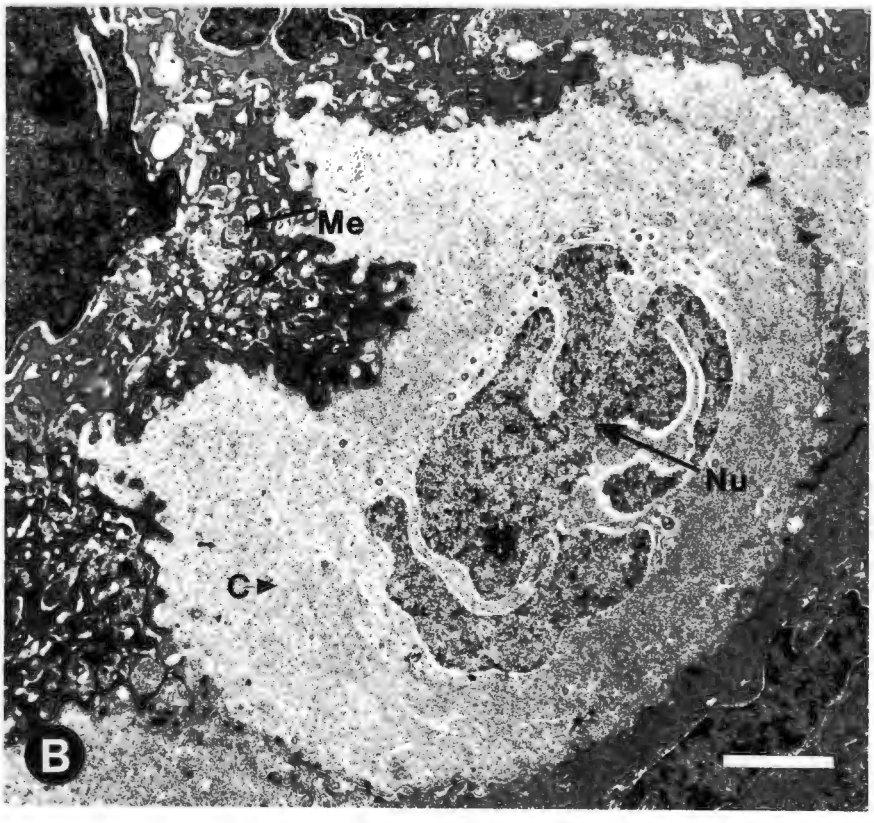
Me
Nu
C
B

Figure 10.4 **Transmission electron micrograph of the rabbit corneal epithelial layer after 3 hours exposure to UV-B radiation, followed by 3 hours recovery showing some of the ultrastructural abnormalities**

Some unusually large space (Sp) formations can be seen between adjacent cells of the inner cell layer. A dead cell (De) almost devoid of cytoplasm is located directly beneath another dead cell (Su) on the surface. Several cells of the polyhedral and basal layers appear to have cytoplasm (C) which varies in electron density.
Scale represents 2 μm. Mag 5200x

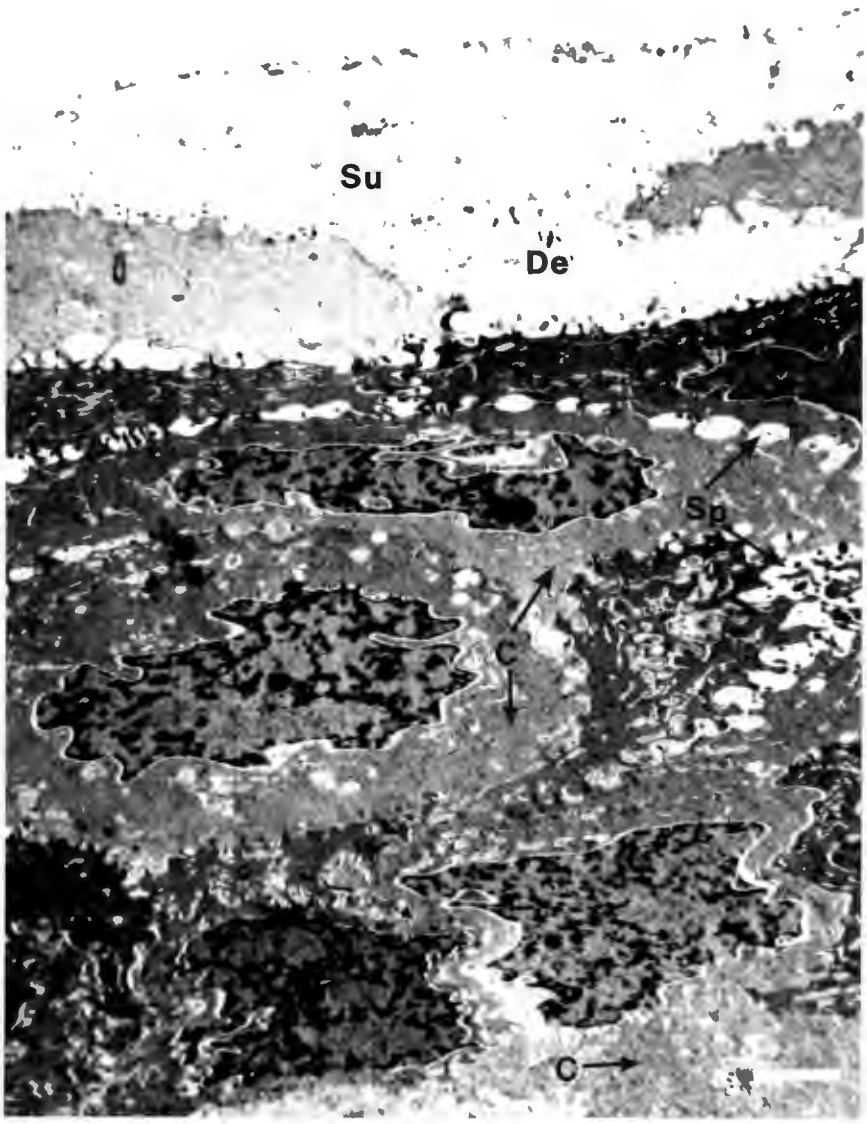
Su
De
Sp
C
C

Figure 10.5 **Transmission electron micrographs of the rabbit corneal epithelial layer after 3 hours exposure to UV-B radiation followed by 16 and 21 hours recovery which show some of the long term effects of the radiation**

A) Some membraneous (Me) vesicles can still be seen in the lower cell layer after 16 hours recovery. The squamous (Sq) layer appears to have regained its normal 3 to 4 cell layer. A single dead (De) cell ready to be discarded is seen on the surface.
Scale represents 2 μm. Mag 5400x

B) Cross section through the epithelium following 21 hours of recovery shows the cells to be tightly knit with well defined nuclei (Nu) and apparently fewer vesicles.
Scale represents 2 μm. Mag 5200x

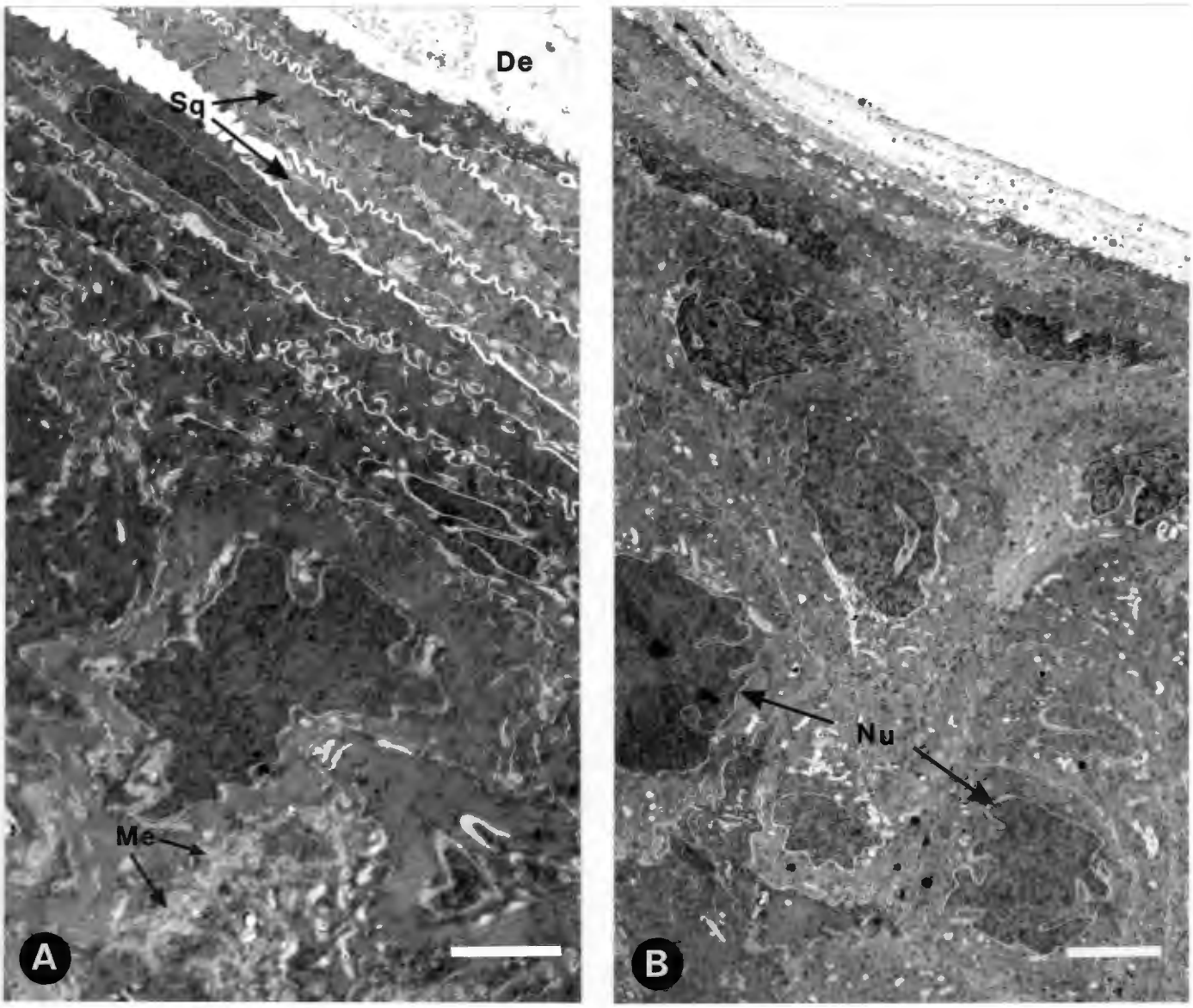
De
Sq
Me
A
Nu
B

Figure 10.6 **Transmission electron micrographs of the rabbit corneal epithelial layer after daily chronic exposure for 119 and 144 days showing some of the effects of accumulative exposure over a longer period of time**

A) Membrane (M) fragments were observed in several of the epithelial cells after 119 days of accumulative exposure to ultraviolet B radiation.
Scale represents 1 μm. Mag 5200x

B) Vacuole like structures (V) were found to occupy most of the cells in the epithelial layers after 144 days of accumulative exposure. The cytoplasm (C) of many of the cells appears non uniform and patchy.
Scale represents 2 μm. Mag 8000x

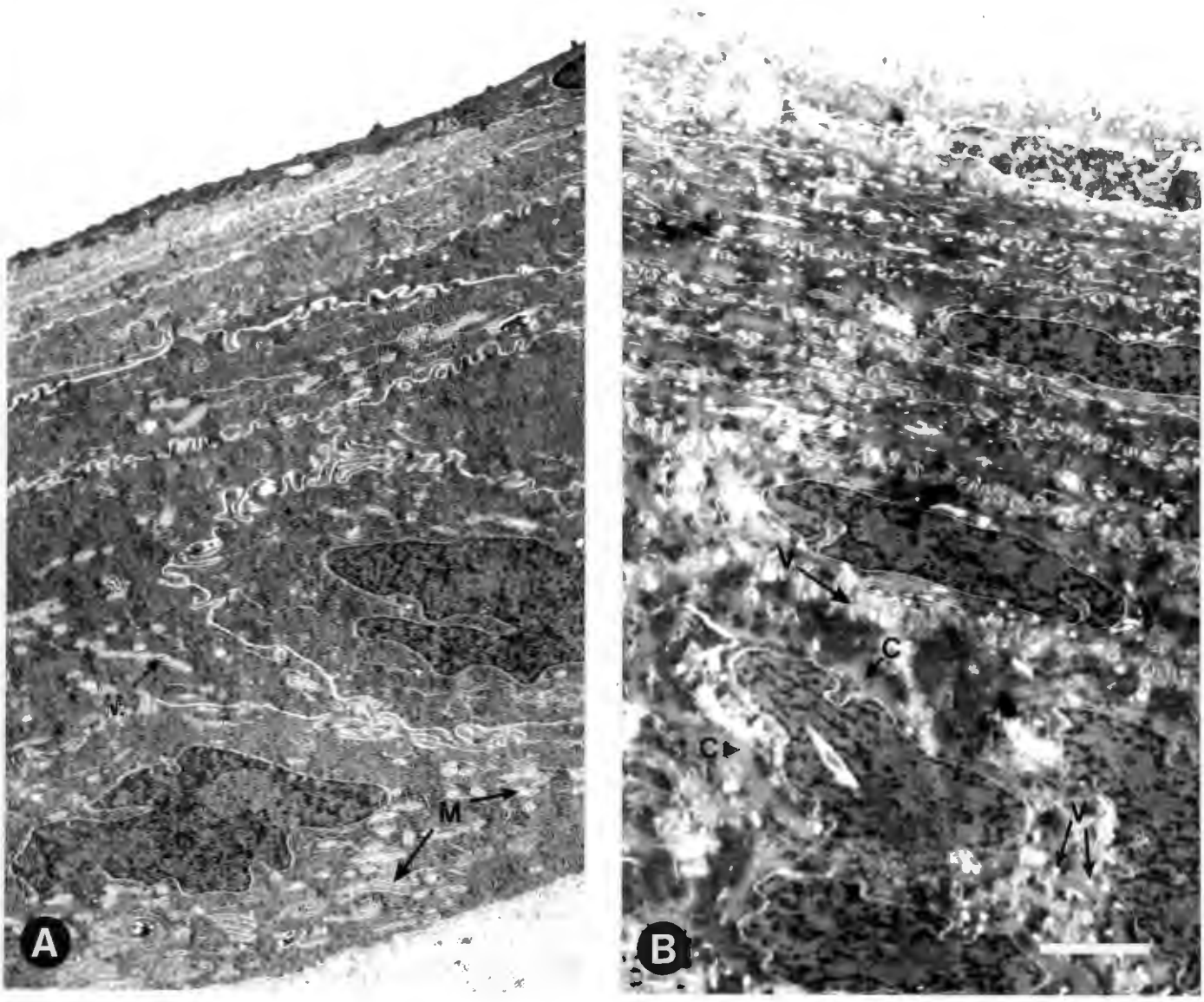
M
A
V
C
C
V
B

DISCUSSION

8.1. Scanning and transmission microscopy of the normal rabbit cornea

The appearance of the rabbit cornea as seen by scanning electron microscopy in this study closely corresponds to that observed by other researchers using rabbit cornea, (Hoffman, 1972; Pfister, 1973 and Ringvold, 1983). The characteristic "light", "medium" and "dark" cells could easily be identified as could the ring-shaped structures, alternately referred to as 'craters' by Hoffman (1972) and 'full-thickness epithelial holes' by Pfister (1973). The consensus on "light", "medium" and "dark" cells is that they are transition stages of the same cell, where the "light" cells are the younger ones, while the "dark" cells are the older ones (Pfister, 1973).

It should be noted that the terminology of "light", "medium" and "dark" is a result of the density of the secondary electron emission from the cell surface which in turn is dependent on the different number and the patterns of surface microvilli. For example, the "dark" cells have roughly twice as many microvilli per square micron as the "light" cells (Pfister, 1973) but due to the shorter length of the "dark" cell microvilli and that they are most likely covered with a thicker layer of mucin, their yield of secondary electrons is less and thus appear "dark". The "light" cells on the other hand have on average longer microvilli, are fewer in number per unit area and covered with a thinner coat of mucin. This means they are more prominent from the surface and yield a "brighter" image due to an increased

yield of secondary electrons.

As an animal model the rabbit corneal epithelial layer is ideal for studying the effects of ultraviolet radiation for a number of reasons: 1) the epithelial cells are uncovered except for a thin rather transparent tear film which does not provide much of a barrier to ultraviolet radiation, 2) the rabbit is small and easily handled, 3) the cells are easily exposed in an experimental setup, 4) the surface cells are characteristically "light", "medium" or "dark" and their surface distribution in the normal rabbit cornea is well defined. The surface epithelial cells are constantly being replaced, a normal process of exfoliation which sees young cells being pushed to the surface to replace the older cells which are eventually discarded. In addition almost all previous research on the effects of UV radiation on the eye have used the rabbit, therefore use of the rabbit as an animal model would allow comparison of any new data with earlier data.

As well as the "light", "medium" and "dark" appearance of the surface epithelial cells one could also see bright droplet-like globules spread out over the surface of the epithelial cells (Fig. 8.3). These globules are most probably pieces of the mucin layer, a layer which covers the epithelial cells and imparts some added thickness. According to Pfister (1973) this mucin layer obscures surface detail, specifically the microvilli and could lead to a misinterpretation that the microvilli are actually surface ridges. Pfister (1973) was specifically interested in the adhesive properties of the tear film and the integrity of the tear film during epithelial exfoliation, which required that the

mucin layer be removed for his methods. It was not the purpose of our study to examine any specific details of the surface microvilli nor their interaction with the tear film, hence treatment to remove the mucin layer was left out in our study. Had we removed the mucin layer, the surface characteristics of the epithelial layer might well have been altered and put in question the validity of using the rabbit cornea as an animal model in studying the effects of ultraviolet radiation.

Instead, very careful attention was paid to the entire corneal processing technique and subsequent coating in order to minimize any possible surface artifacts. For example, in this study the surface epithelial layer in the control cornea (Fig. 8.1 A) appears very flat, much more so than the SEM images recorded by Hoffman (1972). The SEM micrograph of his control cornea show surface cells with the nuclei buldging out slightly and the surface somewhat uneven. This is probably because the cornea in the study by Hoffman (1972) was most likely vacuum or air dried, a suggestion put forward by Pfister (1973). This assumption is further confirmed when one compares the normal epithelial layer of this study (Fig. 8.1 A) with the SEM micrograph of a similar cornea in the study by Ringvold (1983). The appearance of the epithelial layer seen by Ringvold (1983) who used the critical point drying technique, closely resembles those in this study, namely flat with no raised nuclei. In order to be able to characterize early morphological changes attributable to ultraviolet radiation it is obvious that the SEM image of the epithelial layer must appear as flat and true as possible, closely resembling the natural state.

Another distinctive characteristic of the normal epithelial layer are the abundant ring-shaped structures present on the surface epithelial cells. The ring-shaped structures were also observed by (Hazlett *et al*, 1980), Pfister (1973), Hoffman (1972) and Ringvold (1983) and are a distinct feature of the normal rabbit corneal epithelial layer. These features were also found on the corneal epithelial cells of the other animal cornea examined by Pfister (1973). He noted that the structures seemed to occur more frequently on the rabbit cornea than on the cat, dog or monkey though exact numbers were not reported. He also noted that many "dark" cells had these structures while only occasionally did the "light" and "medium" cells contain ring-shaped structures. A plausible explanation for these many holes on "dark" cells comes from Pfister (1973). He proposes that they are part of a "dark" cell's pattern of exfoliation whereby the normal "dark" cell is thought to develop a depression or elevation in the plasma membrane which then breaks through to form a 'crater'. As soon as this hole breaks through and enlarges in the "dark" cell, well developed microvilli from an underlying "light" cell are visible in the hole. This filling in process of the young cell is necessary to maintain the integrity of the tear film. These features were also visible in our study on the normal rabbit control cornea.

In order to try and verify some of our results obtained with the SEM, we also undertook a study to investigate probable cellular changes with the TEM. This procedure had the additional advantage that we could also look at apparent cellular changes in the deeper layers of the corneal epithelium. The anatomical

features of the rabbit corneal epithelium have been well documented by transmission electron microscopy, (Aano, 1961; Blumke, 1967; Hazlett *et al.*, 1980). Cytologically, the epithelium is a densely packed cellular layer divided into three distinct cell layers where the closely knit cells show little actual or artefactual intercellular spaces. The normal epithelium also does not contain any blood vessels or leucocytes. At the ultrastructural level the cytoplasm is sparse in organelles though mitochondria, Golgi apparatus and endoplasmic reticulum can be seen in the cells of all three layers. However, the squamous cells as they approach the surface of the cornea become increasingly thinner and appear to contain fewer organelles. Other cellular features, such as, membrane-bound dense bodies and vesicles have also been observed. Irregular shaped nucleoli are often found in the nuclei of the cells in all three layers.

This pattern is consistent with the normal process of exfoliation in the corneal epithelium. It involves the gradual migration of the innermost basal cells to the surface and in doing so the cells become increasingly flatter, thinner and wider until they reach the surface.

8.2 Scanning and transmission microscopy of the acute effects of ultraviolet radiation

The changes that occur to the corneal epithelial layer after exposure to nonionizing radiation are very complex and it is this ionizing radiation which interacts with the molecules that make up the tissues. In a complex biomolecule the part that absorbs the photons and which is excited is known as the

chromophore. The chromophore may act as a store of energy which is available for rearranging bonds and driving reactions. The chromophores are functional groups joined, for example, to protein chains and are usually aromatics (Marshall, 1991).

Proteins are molecules of great abundance in the corneal epithelium and over 99% of the chemical composition of the cornea is composed of molecules that contain chromophores absorbing only in the UV regions between 200 and 295 nm (Lerman, 1984). Proteins are built of chains of amino acids and the absorbing properties of a protein are largely the sum of the absorptions of its individual amino acids. In the corneal epithelium the amino acids of tyrosine and tryptophan are the principal absorbers at 288 to 290 nm due to the aromatic residues they contain.

It is known that only absorbed radiation can cause a photochemical reaction and all the protein molecules which contain chromophores are characterized by a particular absorption spectrum. Since certain molecular species can only absorb radiation of certain wavelengths, the emission spectrum of the radiation source must include the absorption spectrum of the chromophore. The absorption spectra of small molecules are reasonably narrow, while large molecules like DNA have a broad absorption spectrum because the large molecule has a variety of atoms and bonds within the molecule (Lerman, 1984). Once the radiation has been absorbed, certain photochemical changes may occur in the chromophore and this then eventually leads to an observed biological response. The actual biological response is probably brought about by changes in cell and tissue function with the participation of certain mediators. If the chromophore

is known, the wavelengths of radiation used to initiate a biological response can be specific to the absorption spectrum of the molecule. If the chromophore is unknown, which is usually the case, then the action spectrum for the biological response is determined first by testing the magnitude of the response at various wavelengths.

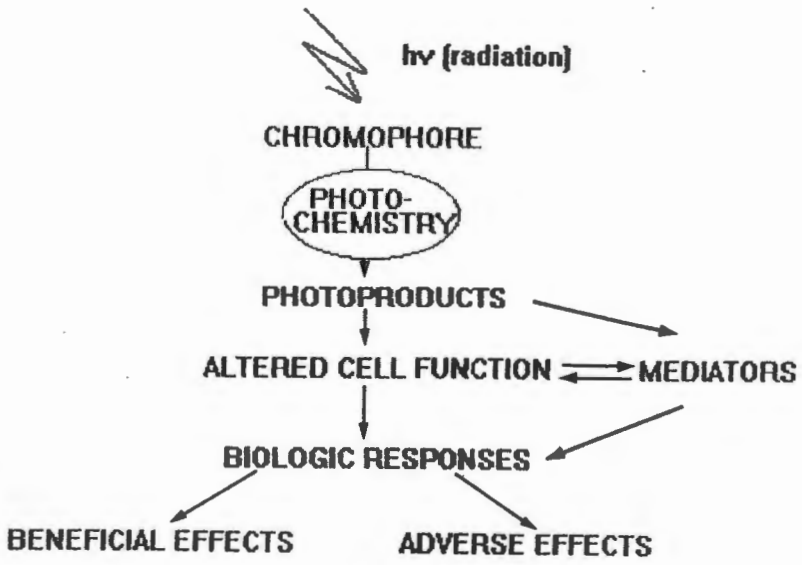

Figure 11.1 A possible sequence of events occurring after exposure to nonionizing radiation from Morison (1984).

In our acute experiments, the rabbit cornea were subjected to a radiation dose calculated to be 0.31 Jcm^{-2} based on a radiometer measurement of 28.8 $\mu W/cm^2$ (TABLE IV). This level of radiation is a factor of 20 above the threshold level of 0.0156 Jcm^{-2} determined by Pitts *et al* (1969), which is therefore more

than enough to induce photokeratitis. Other researchers used radiation doses higher than our levels, these include: Pitts *et al* (1969) who used 0.60 Jcm^{-2} and Cullen (1980b) who used a level as high as 1.0 Jcm^{-2}.

The SEM micrographs of the cornea exposed for 3 hours with a collective dose of 0.31 Jcm^{-2} show clearly how badly the epithelial layer can be damaged by this treatment. From the micrographs in Figs. 8.4 and 8.5 it is obvious that the radiation has brought about substantial morphological changes to occur in the surface epithelial cells which include: severe bulging of the superficial cells most probably due to cellular oedema, holes extending deep into the epithelial layer, rupture of the surface membrane exposing the nucleus to the surface, apparent separation of individual cells and a rapid increase in the desquamation process.

It is interesting to note that these morphological changes are observed immediately after the 3 hour exposure period. By comparison, the clinical picture of photokeratitis, a corneal inflammation reaction (Diffey and Langley, 1986), generally follows a latent period varying somewhat inversely with the amount of exposure. The latent period may be as short as 30 minutes or as long as 24 hours. During the latent period, no signs or symptoms of the radiation damage are evident. Since the latent period varies inversely with respect to the total radiant exposure, higher levels of radiation exposure reduce the latent period, with a response occurring within possibly 30 minutes. This would explain why we observed the most morphological damage in the cornea removed after a 3 hour exposure. The latent period

could have occurred after the first hour or two hours of exposure which means the radiation dose was high enough to reduce the time of the latent period to some time period less than the 3 hour exposure time. The actual length of the latent period in our acute experiments is not known. It has been reported that corneal signs began to appear at 3 to 4 hours after exposure to threshold or slightly higher exposure levels Duke-Elder (1926). Full development of photokeratitis probably coincides with the time when the epithelial layer has become totally desquamated which could take as long as 3 to 4 days. Total desquamation was not observed in our experiments as our maximum recovery period was 21 hours. It is important to note that the intensity of UV radiation generally required to induce experimental photochemical change is much higher than is ordinarily encountered in the world. However, the levels used in our experiments (0.31 Jcm^{-2}) could be achieved or exceeded while sunbathing on the beach or snow skiing if ocular protection was not worn.

The severe bulging or rounding out of the superficial epithelial cells was also observed by Ringvold (1983) though in his study this occurred 3 hours after exposure to only 15 minutes of radiant energy. Unfortunately Ringvold (1983) doesn't define his radiant exposure values, instead he states only that the source to subject distance is 50 centimetres hence, comparison of results is difficult. Ringvold (1983) referred to these rounded out cells as "spheroid bodies". If one compares the SEM micrographs of Ringvold (1983) to the micrographs in Fig. 8.4 and 8.5 of this study they appear very similar, though the former show several cells that appear to be charging significantly. This

is an artefact caused by the buildup of an electron charge on the specimen surface. Inadequate coating or the use of too high a probe current are two conditions which can cause such charging. In this case the charging is probably due to the use of evaporation as a coating technique, which we now know is a poor way of coating specimens for scanning electron microscopy. Other morphological damage such as the deep surface holes and the nuclei lying exposed on the surface were not reported by other researchers, probably because the conditions of exposure between this study and that of others are so different.

It was anticipated that the damage seen on the surface with the SEM would extend into the deeper layers of the epithelium since these cells would be subjected to the incident radiation and absorb a good portion of it (Boettner and Wolter, 1962); (Kinsey, 1948). Some damage to the deeper layers was evident though severe damage similar to that of the surface was not readily apparent. Clearly, the number of cell layers had been reduced (Fig. 10.3 A) and the epithelium overall appears to be thinner probably due to the increased fall off of the superficial cells. This observation was also supported by Pitts (1987) and Cullen (1980) who found that after ultraviolet induced damage there was a reduction in the number of cells in the superficial layer. Under extreme conditions (0.60 Jcm^{-2}) a complete loss of the superficial layers occurred. In accordance with the study by Cullen (1980), the cells in the polyhedral layer are selectively affected by ultraviolet radiation and abnormal cells are often found surrounded by cells which appear morphologically normal (Figs. 10.3). Another sign of damage was the degeneration of the

cytoplasm and nuclear material in a few of the polyhedral cells (Figs. 10.3). This degeneration may well be an indication of ultraviolet induced autolysis. Cullen (1980) observed autolysis of polyhedral and deeper superficial cells at near threshold to intermediate levels of ultraviolet exposure. It is interesting, yet peculiar, that in our study there were no visible lysosomes in any of the epithelial cells after acute exposure to ultraviolet radiation. Both Cullen (1980) and Pitts (1987) reported the presence of lysosomes much larger in size in the cells of the epithelium particularly the inner polyhedral cells. One possible explanation is that the particular tissue sample selected from the excised cornea in our experiment may not have received sufficient radiation to induce lysosomal formation. It is known that the absorption characteristics of living tissue is complicated and in the case of the cornea, orientation, scatter and other optical phenomena add to this complication. It is also possible that differences in radiation sources and/or experimental methodology might explain why no lysosomes were present in our study.

8.3 Scanning and transmission microscopy of recovery periods following acute exposure to ultraviolet radiation

In addition, we also used the rabbit model to look at possible regenerative changes to the damaged epithelial cells by allowing the cells to recover from radiation damage for varying amounts of time. By observing regenerative changes over a period of time, possible recovery patterns or processes may be

identified which could be useful in predicting the recovery of similar human diseases. In one experiment, when the tissue was allowed to recover for 3 hours after an initial 3 hour dose of radiation, we observed several cracks on the membrane surface of many cells (Fig. 8.6 B). These are probably signs of membrane deformation brought about by the ultraviolet radiation. Ringvold (1983) described similar changes to the superficial corneal epithelial cells of adult albino rabbits following exposure to UV radiation for 15 minutes. It was therefore surprising that we did not see these membrane defects in our previous experimental cornea where the cornea was removed immediately after exposure. It is possible that the appearance of these membrane defects is a time dependent phenomenon occurring some time after damage has occurred. Since the exposure dose and duration of irradiation in our experiments were quite different from those of Ringvold (1983), direct comparison is difficult. When present, the cracks were visible on both the desquamating and non-desquamating cells. According to Ringvold (1983) the defects are most likely a direct result of UV-B radiation since they are lacking in a cornea irradiated through ordinary window glass which roughly excludes wavelengths below 350 nm.

In a second experiment the cornea was allowed to recover for 16 hours after the same initial exposure dose of 0.31 Jcm^{-2}. An increased number of cells are still being discarded as the cornea continues to repair itself. The surface appears much smoother with less cellular bulging and the surface membrane defects seen so clearly in the previous 3 hour recovered cornea are not easily visible. It is known that the cornea is the principal

absorber of UV radiation below 320 nm (Boettner and Wolter, 1962). This would lead us to expect that the underlying polyhedral and basal layers of the epithelium have been damaged by the absorbed radiation and those cells after 16 hours would only now be reaching the surface. These cells having already been damaged would most probably be quickly discarded. Evidence that suggests this to be true is that several "light" cells are seen peeling away prior to being discarded. In the normal process of cell exfoliation it is mainly the "dark" cells which are in the process of being discarded, the "light" cells are young cells which have just reached the surface.

In a third experiment the cornea was allowed to recover for 21 hours. The reappearance of the ring-shaped structures was the most noticeable change after 21 hours recovery, an indication that the epithelial layer may be recovering from the radiation damage. The number of ring-shaped structures decreased significantly after 3 hours exposure. Similarily, Ringvold (1983) noted that after 30 minutes exposure to UV radiation the most striking feature was that these ring-shaped structures were lacking. The further high ratio of "dark" cells to "light" cells is another indication that the damaged cells are being replaced quite rapidly. Light microscope studies have shown that minor corneal damage healed rapidly, and severe radiation damage resolved within 7 days (Cullen, 1980). In fact early work by Duke-Elder and Duke-Elder (1929) showed that epithelial changes became most noticeable at 12 hours, and that abnormal conditions gradually disappeared until 7 days when the cornea appeared essentially normal.

The results from the correlative TEM micrographs of the recovery periods are not conclusive though after a 3 hour recovery period the cells in the squamous layer did show some unusual intercellular spaces which were not present in the control cornea. The results of the 16 hour and 21 hour recovery periods are equally inconclusive and any perceived damage would be highly subjective. It is recommended that a further ultrastructural study of recovery periods be done in more detail before any direct comparison to the SEM results is attempted.

8.4 Scanning and transmission microscopy of the chronic effects to ultraviolet radiation

The main emphasis of this study was on the acute effects of UV exposure. Towards the end of this study we did look at some interesting effects of chronic exposure and these results, although preliminary and of an exploratory nature have been included in this report. Generally, most investigations into pathological effects of abnormal levels of irradiation have focused on the lens and retina. One reason for this could be because the corneal epithelium has excellent regenerative powers and sustained damage is incurred infrequently. However, there is now more interest into the effects of low level exposure over a prolonged period because of the concern that increased levels of harmful ultraviolet radiation is reaching the earth's surface. Recent data on the destruction of the ozone layer has raised concerns that more of the harmful UV-B and UV-C radiation is getting through "holes" in the ozone layer. In addition to "holes" in the ozone layer any decrease in the thickness of this

layer would causes large changes in the levels of ultraviolet radiation reaching the earth's surface. This occurs because the absorption of ultraviolet radiation by the ozone layer is an exponential function in that a small number of ozone molecules absorb a large amount of ultraviolet radiation.

To study chronic effects we exposed the rabbits to a daily low level dose of radiation of 0.008 Jcm^{-2} (TABLE IV) for the first 106 days and then increased the dose to 0.016 Jcm^{-2} for the remaining 12 days. It was decided to increase the dose because it was felt that at one half of threshold (0.008 Jcm^{-2}) this daily amount of radiation would be too low to yield clear effects. Also we irradiated the eye only once per day and then the cornea would have had 22 hours to recover before the next exposure. Unfortunately we were not able to perform controlled step-wise increases in dosage, a limitation when using fixed fluorescent lamps.

The results from the first chronic experiment (Figs 9.1) show that under these conditions of exposure there were some apparent effects on the epithelial cells. Firstly, the slightly raised cell nucleus is a morphological indication that some trauma has occurred probably a result of accumulative radiation over 119 days. Secondly, many more of the "light" cells (Fig 9.1 B) show ring-shaped structures on their surface which indicates that they are beginning the process of desquamating. This is unusual since in the normal process of exfoliation it is mainly the "dark" mature cells about to be discarded which exhibit the majority of these ring-shaped structures. It is possible that these "light" young cells have been damaged by the radiation

prior to reaching the surface and begin the process of exfoliation by forming ring-shaped structures just as they reach the surface. It was Pfister (1973) who first suggested that the normal pattern of exfoliation is thought to occur when a dark cell develops a depression or elevation which then progresses into a ring-shaped structure. As soon as the hole breaks through the surface dark cell, the well-developed microvilli from an underlying "light" cell are visible. Eventually the hole enlarges and the cell is discarded and the young cell underneath fills in the space of the discarded "dark" cell.

Other researchers, namely Zuclich (1980) and Cullen (1980) have reported on the additive effects of ultraviolet radiation. For example, Cullen (1980) observed that if rabbit cornea was irradiated with half-threshold levels of UV radiation, any minor damage to the cellular elements undergoes sufficient repair rapidly. Accordingly the cornea can withstand additional trauma after 4 hours. It should be noted that the conclusions drawn by Cullen (1980) were based on light and electron microscopic observations. The study by Zuclich (1980) does not relate directly to our experiments since he used monochromatic radiation at 350 and 356 nm, a range which forms part of the absorption tail of the cornea. Although the absorption tail of the cornea does stretch into the UV-A band its absorption drops off quite rapidly above 300 nm.

The results indicate that even a sub-threshold dose of UV-B radiation administered over a long enough period has an accumulative effect which can be seen with the scanning electron microscope.

On the other hand, the effects of longer (144 days) and higher (0.112 Jcm^{-2}) chronic exposures are much more evident (Figs 9.2). Morphological damage to the superficial layer is evident from the many cells peeling away, the prominent bulging of some of the cell nuclei and the formation of cracks between cells. In fact, irradiation damage to the epithelial layer was very similar to what was found by acute exposure. It should be noted that the exposure dose of 0.112 Jcm^{-2}, while above threshold, was still less than in the acute experiments. It appears that the cornea has not had sufficient time to recover between the daily doses in our experiments and the accumulative effects such as; slightly raised cell nuclei, few if any ring - shaped structures and cracks between adjacent cells were clearly visible.

The scanning electron microscopy of the acute experiments did show positive changes to the surface epithelial cells and the damage was easily recognized. The recovery periods did follow a logical progression though the results were not totally conclusive. The transmission electron microscopy results were less convincing though a more careful ultrastructural study would probably provide some useful information. It was felt that as an animal model, the rabbit cornea is ideal for studying ultraviolet radiation damage. Amongst others, it appears very sensitive to any form of ocular trauma and has distinct surface characteristics which could be useful in the study of disease progression. In this study we only examined the central region of the cornea but in the future it would be of interest to compare the effects of ultraviolet radiation between the central

and peripheral regions of the cornea.

We concentrated our study on the effects of UV-B radiation on the corneal epithelium though UV-B absorption extends to the stroma and the endothelium. A detailed analysis of the effects of UV-B radiation on these two layers was excluded from our study as this would have required the use of many more experimental animals plus a much longer time frame for completion of the study. The effects of ultraviolet radiation on the stroma has been reported by Ringvold and Davanger (1985) and on the endothelium by Ringvold *et al* (1982) and Cullen *et al* (1984).

We believe that our present studies, while providing important evidence for acute effects of UV damage on the cornea, should be extended to address especially the following issues: 1) longer recovery periods 2) better correlation between SEM and TEM and 3) better and more detailed study of chronic effects and 4) significantly examine cytochemical and immunocytochemical changes.

In summary, the corneal epithelium has been studied extensively and a great deal is known about its reaction to ultraviolet radiation. Unfortunately the corneal epithelial layer is a heterogenous structure of varying thickness with great regenerative powers which makes it difficult to apply any absorption data to such a structure.

REFERENCES

Andley, U.P. (1987). Yearly review - Photodamage to the eye. Photochem Photobiol 46, No 6, 1057-1066.

Aono, H. (1961). Electron microscopical studies on the cornea. Folia Ophthal Jap 12, 331-357.

Bachem, A. (1956). Opthalmic ultraviolet action spectra. Am J Ophthalmol 41 (6), 969-975.

Blumcke, S., and Margenroth, K. (1967). The stereo ultrastructure of the external and internal surface of the cornea. J Ultrastruc Res 18, 502-518.

Boettner, E.A., and Wolter, J.R. (1962). Transmission of the ocular media. Invest Ophthalmol 1, 776-783.

Buschke, W., Friedenwald, J.S., and Moses, S.G. (1945). Effects of ultraviolet radiation on corneal epithelium: mitosis, nuclear fragmentation, post-traumatic cell movements, loss of tissue cohesion. J Cell Comp Physiol 26, 147-164.

Cameron, M.E. (1965). Pterygium throughout the world. Springfield, Ill. Charles C. Thomas.

Cogan, D.G., and Kinsey, V.E. (1946). Action spectrum of keratitis produced by ultraviolet radiation. Arch Ophthalmol 35, 670-677.

Cogan, D.G. (1951). Corneal symposium. Applied anatomy and physiology of the cornea. Trans Amer Acad Ophthal 329-359.

Coohill, T.P. (1987). Yearly review - The effects of the ultraviolet wavelengths of radiation present in sunlight on human cells in vitro. Photochem and Photobiol 46, No 6, 1043-1050.

Cullen, A. (1980a). Ultraviolet induced lysosome activity in corneal epithelium. Albrecht von Graefes Arch Klin Ophthalmol 214, 107-118.

Cullen, A. (1980b). Additive effects of ultraviolet radiation. Am J Optom Physiol Optics 54, No 11, 808-814.

Cullen, A., Chou, B.R., Hall, M.G., and Jany, S.E. (1984). Ultraviolet-B damages the corneal endothelium. Am J Optom Physiol Optics 61, No 7, 473-478.

Davson, H. (1990). Physiology of the Eye. 5th edition, McMillan Press.

Diffey, B.L., and Langley, F.C. (1986). Evaluation of Ultraviolet Hazards in Hospital. London: Institute of Physical Sciences in Medicine.

Duke-Elder, W.S. (1926). The pathological action of light on the eye, I. Action of the outer eye, photophthalmia. Lancet 1, 1137-1141.

Duke-Elder, W.S., and Duke-Elder, P.M. (1929). A histological study on the action of short-waved light on the eye with a note on the "inclusion bodies". Br J Ophthalmol 13, 1-37.

Duke-Elder, W.S., (1954). Textbook of ophthalmology. St Louis: Mosby 7, 570-586.

Farrell, R.A., McCally, R.L., and Tatham, P.E.R. (1973). Wavelength dependencies of light scattering in normal and cold swollen rabbit corneas and their structural implications. J Physiol 233, 589-612.

Freedman, A. (1965). Labrador keratopathy. Arch Ophthalmol 74, 198-202.

Friedenwald, J.S., Breschke, W., Crowell, J., and Hollender, A. (1948). Effects of ultraviolet irradiation on the corneal epithelium II. Exposure to monochromatic radiation. J Cell Comp Physiol 32, 161-173.

Giraud, J.P., Pouliqwen, Y., Offret, G., et al (1975). Statistical studies in normal human and rabbit cornea stroma. Exp Eye Res 2 (13) 221-229.

Grayson, M. (1979). Diseases of the Cornea. The C.V. Mosby Co. 191-192.

Gregory, R.L. (1966). Eye and Brain. World University Library, 13-25.

Grossweiner, L.I. (1984). Phtochemistry of proteins: a review. Current eye Research Vol 1, No 1, 137-144.

Hazlett, L.D., Wells, P., Spann B., and Berk, R.S. (1980). Epithelial desquamation in the adult-mouse cornea, a correlative TEM-SEM study. Ophthalmic Res 12, 315-323.

Hill, J.C., and Maske, R. (1989). Pathogenesis of pterygium. Eye 3, 218-226.

Hoffman, F. (1972). The surface of the epithelial cells of the cornea under the scanning electron microscope. Ophthal Res 3, 207-214.

Holly, F.J., and Lemp, M.A. (1977). Tear Physiology and dry eyes. Surv Ophthalmol 22, 69-75.

Kaye, G.I., and Papas, G.D. (1962). Studies on the cornea. J Cell Biol 12, 457.

Kinsey, V.E. (1948). Spectral transmission of the eye to ultraviolet radiations. Arch Ophthalmol 39, No 4, 508-513.

Lerman, S. (1984). Biophysical aspects of corneal and lenticular transparency. Curr Eye Res 3, No 1, 3-13.

Marshall, J. ed. (1991). The Susceptible Visual Apparatus. CRC Press Inc. 37-43.

Maurice, D. (1957). The structure and transparency of the cornea. J Physiol 136, 263-286.

Mollenhauer, H.H. (1964). Plastic embedding mixtures for use in electron microscopy. Stain Technol 39, 111-114.

Morison, W.L. (1984). Phototherapy and Photochemotherapy of Skin Disease. Praeger Scientific, 6-23.

Norm, M. (1984). Spheroid degeneration, keratopathy, pinguecula, and pterygium in Japan (Kyoto). Acta Ophthalmol 62, 54-60.

Olsen, E.G., and Ringvold, A. (1982). Human cornea endothelium and ultraviolet radiation. Acta Ophthalmol (Copenh) 60, 54-56.

Parrish, J.R.R., Anderson, F., Urbach, and Pitts, D.G. (1978). Human Biologic Responses to Ultraviolet Radiation. Plenum Press.

Pfister, R.R. (1973). The normal surface of corneal epithelium: a scanning electron microscope study. Invest Ophthalmol 12, 654-668.

Pitts, D.G. (1970). A comparative study of the effects of ultraviolet radiation on the eye. Am J Optom Arch Am Acad Optom 50, 535-546.

Pitts, D.G. (1973). The ocular ultraviolet action spectrum and prtection criteria. Health Phys 25, 559-566.

Pitts, D.G. (1977). The ocular effects of ultraviolet radiation. Am J Optom Physiol Optics 55, No 1, 19-35.

Pitts, D.G., Kay, K.R. (1969). The photo-ophthalmic threshold for the rabbit. Am J Optom Arch Am Acad Optom 46(8), 561-572.

Pitts, D.G., Prince, J.E., Butcher, W.I., Kay, K.R., Brown, R.W., Casey, H.W., Richey, D.G., Mori, L.H., Strong, J.E., and Tredici, T.J. (1969). The effects of ultraviolet radiation on the eye. SAM-TR-69-10, USAF School of Aerospace Medicine, Brooks AFB, Texas.

Pitts, D.G. and Tredici, T.J. (1971). The effects of ultraviolet on the eye. Am Ind Hgy Assoc J 32, 235-246

Pitts, D.G., Cullen, P., and Hacker, P.D. (1977). Ocular effects of near ultraviolet radiation: Literature review. Am J Optom Physiol Optics 54, No 8, 542-549.

Pitts, D.G., Bergmanson, P.G., and Chu, L.W-F. (1987). Ultrastructural analysis of corneal exposure to UV radiation. Acta Ophthalmol 65, 263-273.

Ringvold, A. (1980). Cornea and ultravioler radiation. Acta Ophthalmol (Copenh) 58, 63-68.

Ringvold, A., Davanger, M., and Olsen, E.G. (1982). Changes of the cornea endothelium after ultraviolet radiation. Acta Ophthalmol (Copenh) 60, 41-53.

Ringvold, A. (1983). Damage of the cornea epithelium caused by ultraviolet radiation-a scanning electron microscopic study in the rabbit. Acta Ophthalmol (Copenh) 61, 898-907.

Ringvold, A., and Davanger, M. (1985). Changes in the rabbit corneal stroma caused by UV-radiation. Acta Ophthalmol 63, 601-606.

Smolin, G., and Thoft, R.A. ed. (1983). The Cornea: Scientific Foundations and Clinical

Verhoeff, F.H., and Bell, L. ed (1916). The pathological effects of radiant energy on the eye: an experimental investigation with a systematic review on the literature. Pro Am Acad Arts Sci 51, 630-811.

Widmark, E.J. (1889). Uber der Einfluss des Lichtes auf die Vorderen Medien des Auge. Skand Arch Physiol 1, 264-280.

Zuclich, J.A. (1980). Cumulative effects of near-UV induced corneal damage. Health Phys 38, 833-838.

Zuclich, J.A. (1984). Ultraviolet induced damage in the primate cornea and retina. Curr Eye Res 3, No 1, 27-34.